Utilizing NASA's Cold Atom Lab for Precision AI and Control of Ultracold Atomic and Molecular Gases in Space

Jason R. Williams
Quantum Sciences and Technology Group
Jet Propulsion Laboratory, California Institute of Technology, Pasadena, CA

Overview

- Introduction: Precision Atom Interferometers (AI) for fundamental physics research in space.
- Study #1: *Low-energy Feshbach physics to prepare highly-overlapped dual-species atomic gases in microgravity.*
- Study #2: *Technology maturity of precision AIs for fundamental physics studies on the ISS.*

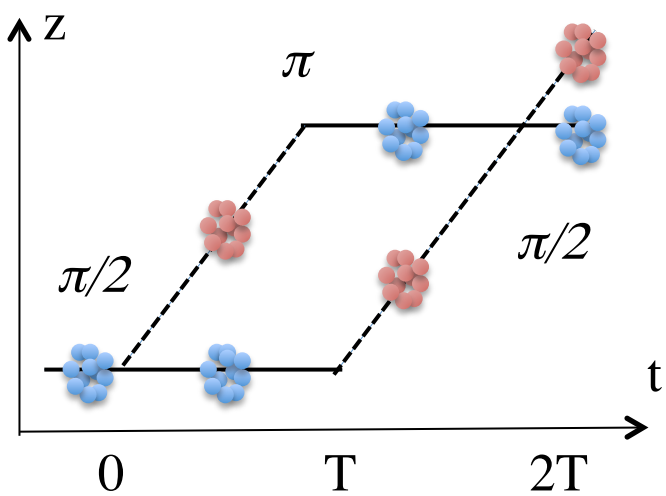

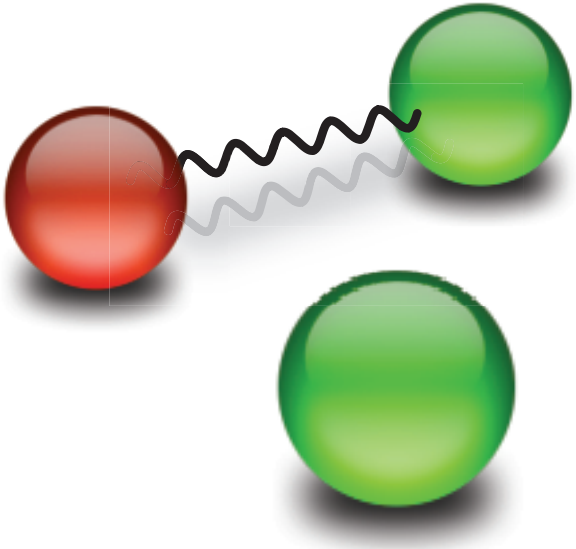

Overview

- Introduction: Precision Atom Interferometers (AI) for fundamental physics research in space.
- Study #1: *Low-energy Feshbach physics to prepare highly-overlapped dual-species atomic gases in microgravity.*
- Study #2: *Technology maturity of precision AIs for fundamental physics studies on the ISS.*

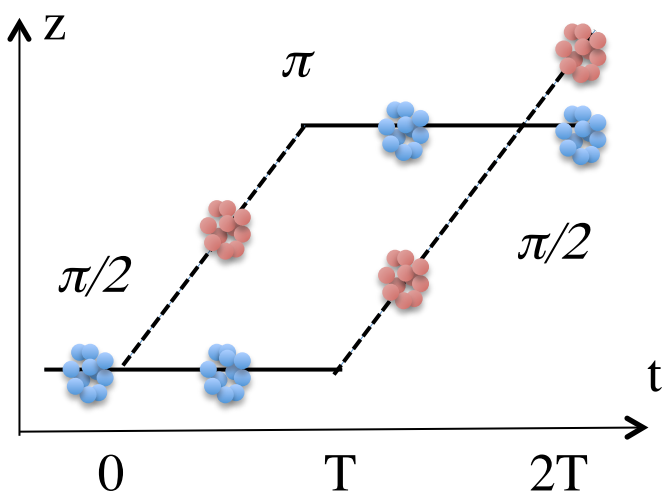

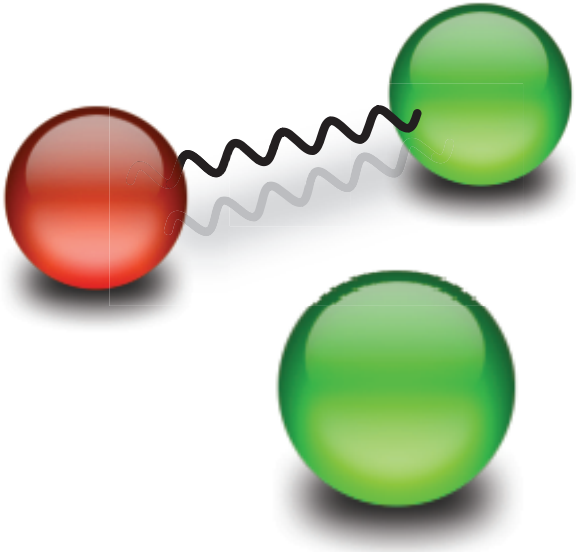

AI Measurements of Fundamental Physics

Wuhan 10m drop tower

PRL 115, 013004 (2015) PHYSICAL REVIEW LETTERS week ending 3 JULY 2015

Test of Equivalence Principle at 10^{-8} Level by a Dual-Species Double-Diffraction Raman Atom Interferometer

Lin Zhou,[1,2] Shitong Long,[1,2,3] Biao Tang,[1,2] Xi Chen,[1,2] Fen Gao,[1,2] Wencui Peng,[1,2] Weitao Duan,[1,2,3] Jiaqi Zhong,[1,2] Zongyuan Xiong,[1,2] Jin Wang,[1,2,*] Yuanzhong Zhang,[4] and Mingsheng Zhan[1,2,†]

Dual-species ^{87}Rb-^{85}Rb AI test of the Weak Equivalence Principle to 3×10^{-8}.

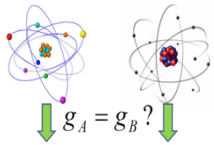

PRL 113, 023005 (2014) PHYSICAL REVIEW LETTERS week ending 11 JULY 2014

Test of Einstein Equivalence Principle for 0-Spin and Half-Integer-Spin Atoms: Search for Spin-Gravity Coupling Effects

M. G. Tarallo,* T. Mazzoni, N. Poli, D. V. Sutyrin, X. Zhang,† and G. M. Tino‡
Dipartimento di Fisica e Astronomia and LENS—Università di Firenze, INFN—Sezione di Firenze, Via Sansone 1, 50019 Sesto Fiorentino, Italy
(Received 24 February 2014; published 8 July 2014)

Dual-species ^{88}Sr-^{87}Sr AI test of the Weak Equivalence Principle to ~ 10^{-7}.

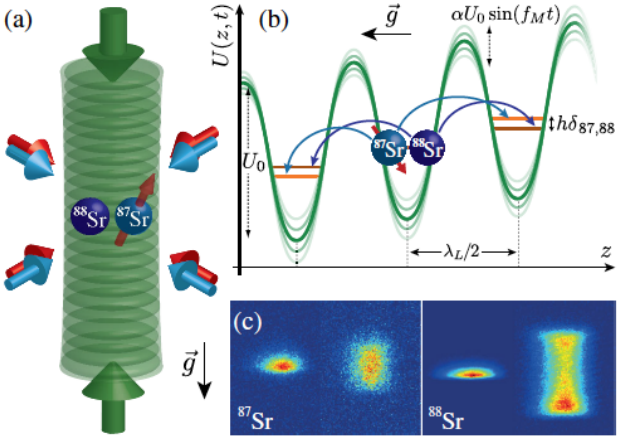

AI Measurements of Fundamental Physics

PRL 103, 050402 (2009) PHYSICAL REVIEW LETTERS week ending 31 JULY 2009

Noise-Immune Conjugate Large-Area Atom Interferometers

Sheng-wey Chiow,[1] Sven Herrmann,[1] Steven Chu,[1,2,3] and Holger Müller[1,2,3,*]
[1]Physics Department, Stanford University, 382 Via Pueblo Mall, Stanford, California 94305, USA
[2]Department of Physics, University of California, 366 Le Conte Hall, Berkeley, California 94720-7300, USA
[3]Lawrence Berkeley National Laboratory, One Cyclotron Road, Berkeley, California 94720, USA
(Received 13 January 2009; published 28 July 2009)

$$\alpha = [(2R_\infty/c)(M/m_e)(h/M)]^{1/2}$$

measured to 3.4 ppb

Fine structure constant,QED

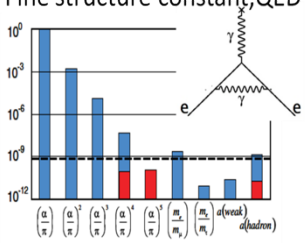

Quantum mass standard

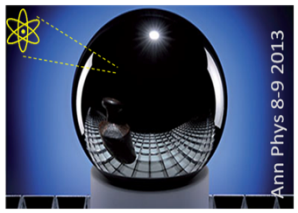

PHYSICAL REVIEW A 91, 033629 (2015)

Testing gravity with cold-atom interferometers

G. W. Biedermann,* X. Wu, L. Deslauriers, S. Roy, C. Mahadeswaraswamy, and M. A. Kasevich†
Physics Department, Stanford University, Stanford, California 94305, USA
(Received 1 December 2014; published 24 March 2015)

For a Yukawa force, the acceleration is given by

$$a_i = \frac{Gm}{r_i^2}[1 + \alpha e^{-r_i/\lambda}(1 + r_i/\lambda)].$$

Constraint on Yukawa-type fifth force at 8×10^{-3} near "poorly known" length scale of 10cm.

Atom-interferometry constraints on dark energy

SCIENCE sciencemag.org
21 AUGUST 2015 • VOL 349 ISSUE 6250

P. Hamilton,[1*] M. Jaffe,[1] P. Haslinger,[1] Q. Simmons,[1] H. Müller,[1,2†] J. Khoury[3]

If dark energy, which drives the accelerated expansion of the universe, consists of a light scalar field, it might be detectable as a "fifth force" between normal-matter objects, in potential conflict with precision tests of gravity. Chameleon fields and other theories with screening mechanisms, however, can evade these tests by suppressing the forces in regions of high density, such as the laboratory. Using a cesium matter-wave interferometer near a spherical mass in an ultrahigh-vacuum chamber, we reduced the screening mechanism by probing the field with individual atoms rather than with bulk matter. We thereby constrained a wide class of dark energy theories, including a range of chameleon and other theories that reproduce the observed cosmic acceleration.

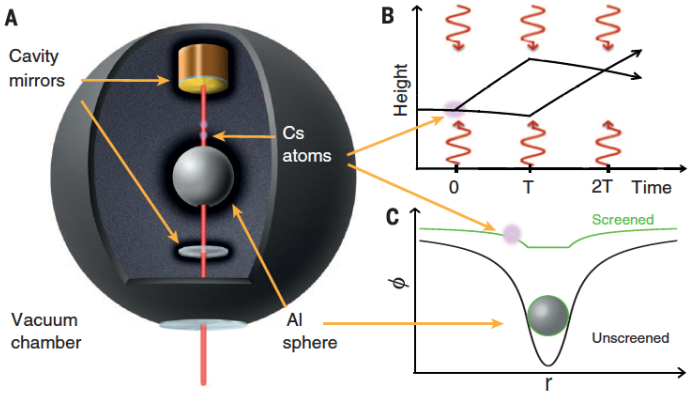

Fig. 1. Screened fields in our experiment. (**A**) The vacuum chamber (radius, 5 cm; pressure, ~6 × 10^{-10} Torr; mostly hydrogen) holds a pair of mirrors forming a Fabry-Perot cavity and the aluminum source sphere. Laser beams pass through a 1.5-mm-radius hole in the sphere (radius of the sphere, 9.5 mm). A Mach-Zehnder interferometer is formed using cold cesium atoms from a magneto-optical trap at an effective distance of 8.8 mm from the sphere surface (not shown). (**B**) Photons in three flashes of laser radiation that are resonant in the cavity impart momentum to the atoms, directing each atomic matter wave onto two paths. (**C**) The potential generated by a macroscopic sphere as a function of distance from the sphere's center.

AI Fundamental Physics in Microgravity

Precision inertial measurements for advancement of science

- Frame-dragging test of the General Relativity Theory
- Test of Einstein's Equivalence Principle with differential acceleration measurements of two atomic species
- Gravitational wave detection
- Spin-gravity coupling with quantized angular momentum states
- Signatures of dark matter and dark energy

Precision measurements of Lense-Thirring effect

Space-**T**ime **E**xplorer and **Qu**antum **E**quivalence **P**rinciple **S**pace **T**est

Light-Pulse Atom Interferometer:

$$\Delta\Phi = 2k\, a\, T^2$$

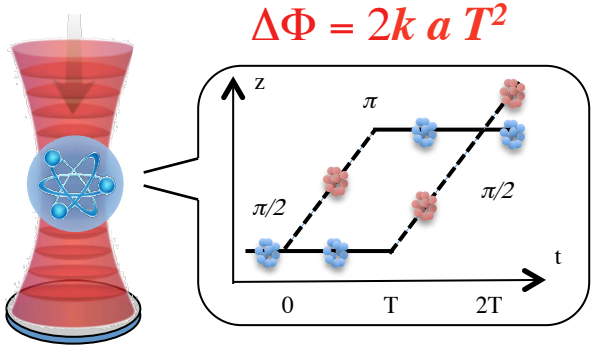

Quantum Test of the Equivalence Principle and Space-Time (QTEST)

State of the art dual-species atom interferometer as a multi-user facility onboard the ISS for:

- Test the Weak Equivalence Principle (WEP) to below 10^{-15} with *quantum* test masses.
- Measure the fine structure constant (α) to 10^{-12} precision for most precise test of QED.
- Most precise primary mass standard in the proposed SI.

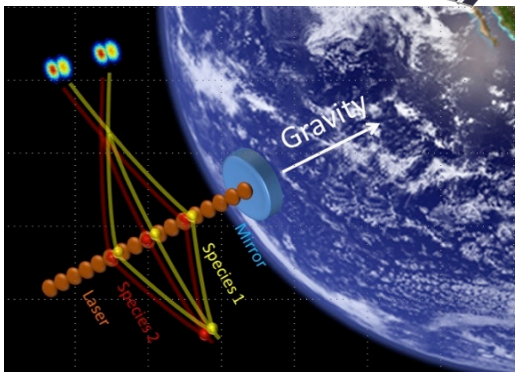

Gravity effects on two different atomic species (^{87}Rb and ^{85}Rb) are compared in space.

Light-pulse MZ Atom Interferometers

- Measurement based on an ensemble of effective 2-level systems, coupled with light pulses with opposite **k**-vectors (Doppler sensitive spectroscopy).
  - Raman pulses couple two electronic and momentum levels, $g_1 \neq g_2$, $k_{eff} = 2k$
  - Bragg pulses couple two momentum levels, same electronic, $g_1 = g_2$, $k_{eff} = 2nk$

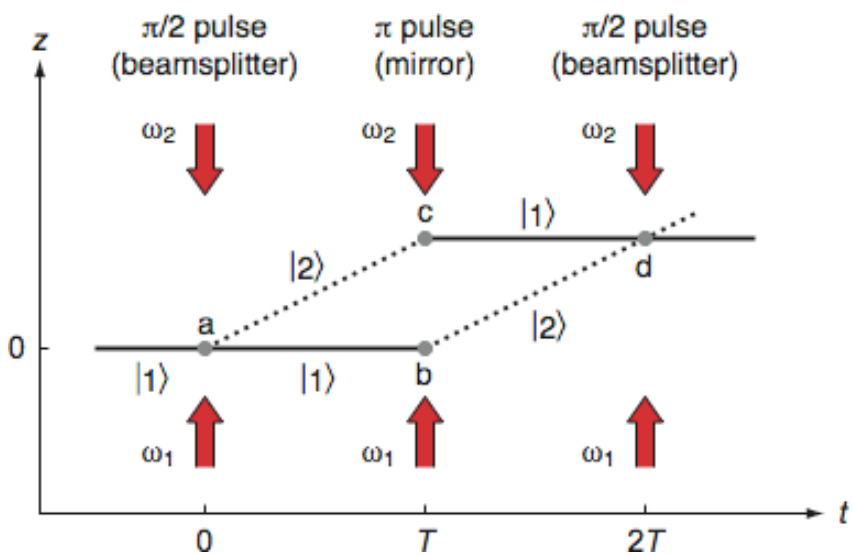

Fig. 1. Light-pulse atom interferometer diagram

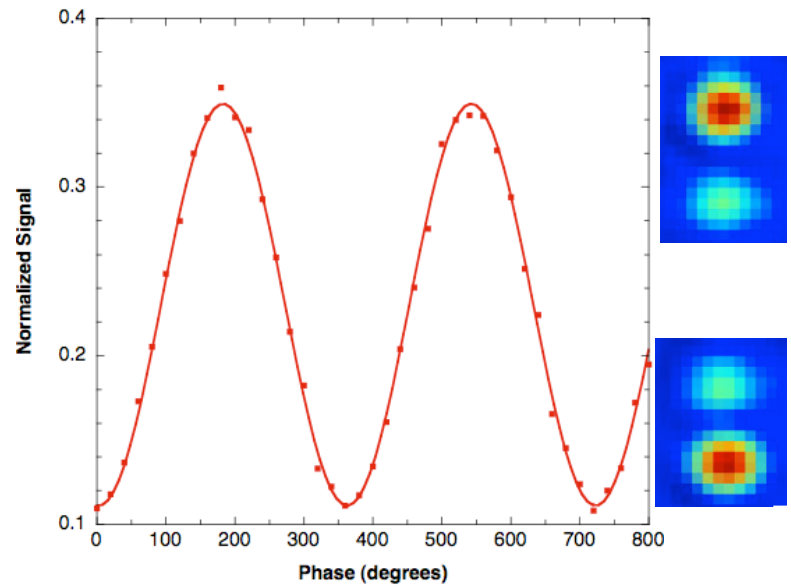

Fig. 2. Atom interferometer fringes as observed in our laboratory prototype instrument [6]. The phase of the final Raman π/2 pulse was scanned to generate the characteristic interferometer fringe.

Sensitive to inertial forces and rotations

$$\Delta\Phi_a = k_{eff} \cdot aT^2$$

$$\Delta\Phi_{rot} = 2m(\Omega \cdot A)/\hbar$$

Simple phase readout from final atomic states:

$$P = \frac{1}{2}(1 - \cos(\Delta\Phi))$$

Differential AI Measurements

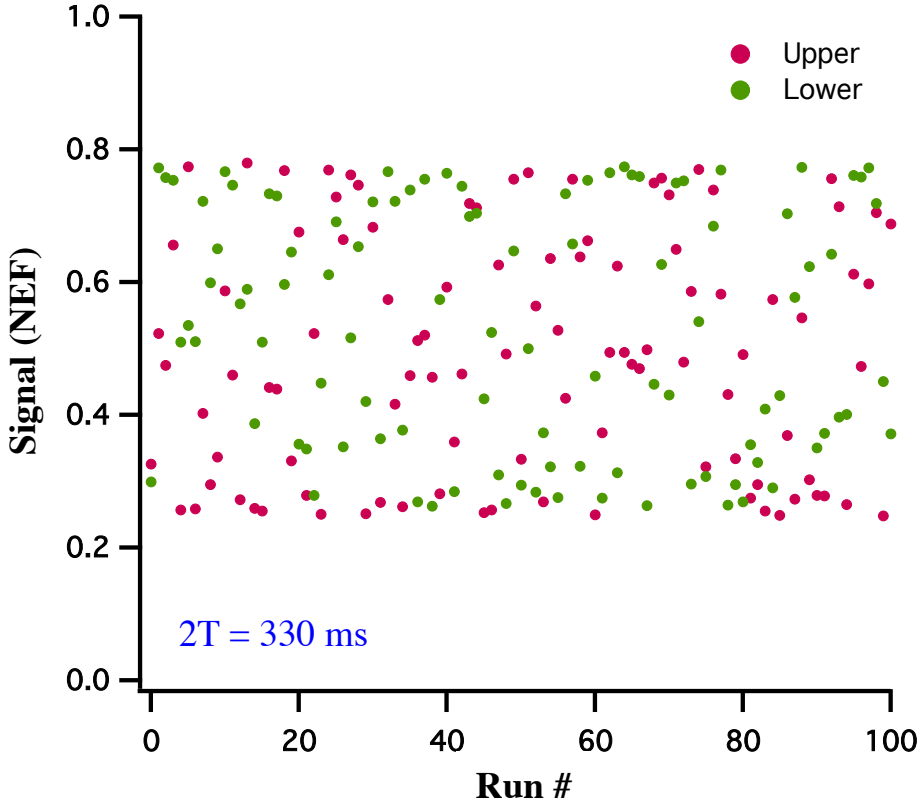

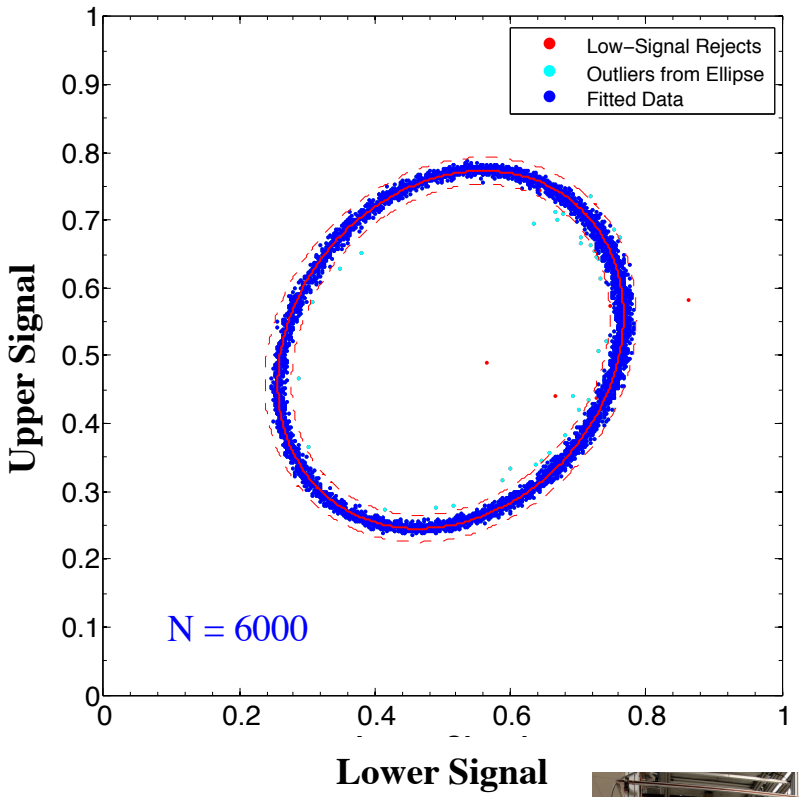

Left: Interferometer fringes for the two chambers of the gravity gradiometer.

Right: Parametric plot of correlations in the atom interferometer signals.

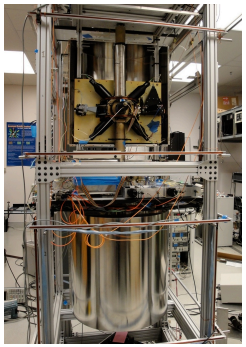

Challenges for Long-T Interferometers

Known sources that can limit the ultimate accuracy include: vibrations, rotations, accelerations, magnetic fields, differential center-of-mass position and velocity, ...

Assuming δv=1μm/s, δz=1μm, $\delta\Omega=10^{-3}\,\Omega_{ISS}$, a = 100 a_0, n_0 = 2 x 10^8/cm^3, 2T = 20s

Gravity gradient shifts

- Test masses traveling different classical paths (δr, δv) experience different gravitational potentials.

$$k_{eff}\gamma_{ZZ}(\delta z+\delta vT)T^2 = 3.0\times10^{-12}\,g$$

Rotations (centrifugal and Coriolis)

- Reduces signal contrast and systematics from different velocities.

$$-2k_{eff}\delta v_z\delta\Omega_y T^2 = 2.6\times10^{-13}\,g$$

Mean-field shift:

- Scales with interaction strength and beam-splitter efficiency/noise (Δp).
- Fundamental density limit.

$$(4\pi\hbar a_{ij}/m)n_{j0}\Delta pT = 3.8\times10^{-13}\,g$$

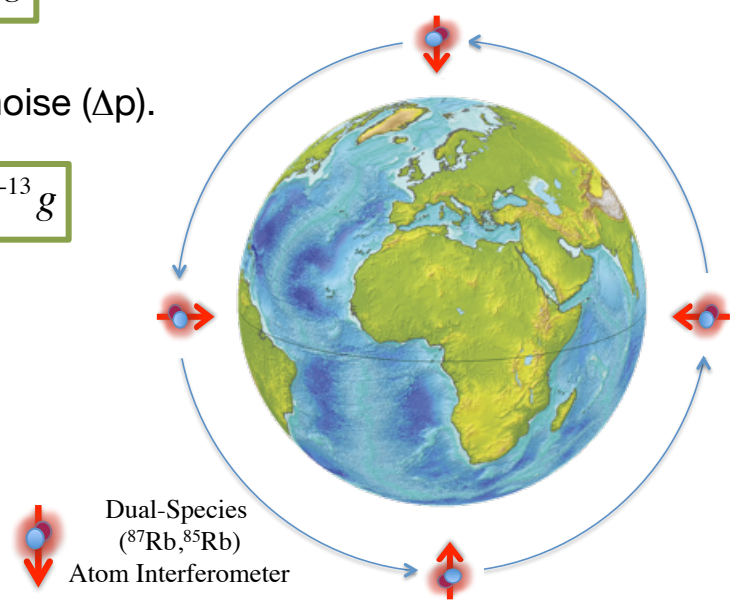

Challenges for Long-T Interferometers

Known sources that can limit the ultimate accuracy include: vibrations, rotations, accelerations, magnetic fields, differential center-of-mass position and velocity, ...

Assuming δv=1μm/s, δz=1μm, $\delta\Omega=10^{-3}\,\Omega_{ISS}$, a = 100 a_0, n_0 = 2 x 10^8/cm^3, 2T = 20s

Gravity gradient shifts

- Test masses traveling different classical paths (δr, δv) experience different gravitational potentials.

$$k_{eff}\gamma_{ZZ}(\delta z+\delta vT)T^2 = 3.0\times10^{-12}\,g$$

Rotations (centrifugal and Coriolis)

- Reduces signal contrast and systematics from different velocities.

$$-2k_{eff}\delta v_z\delta\Omega_y T^2 = 2.6\times10^{-13}\,g$$

Orders of magnitude enhanced cloud overlap necessary for WEP tests.

Mean-field shift:

- Scales with interaction strength and beam-splitter efficiency/noise (Δp).
- Fundamental density limit.

$$(4\pi\hbar a_{ij}/m)n_{j0}\Delta pT = 3.8\times10^{-13}\,g$$

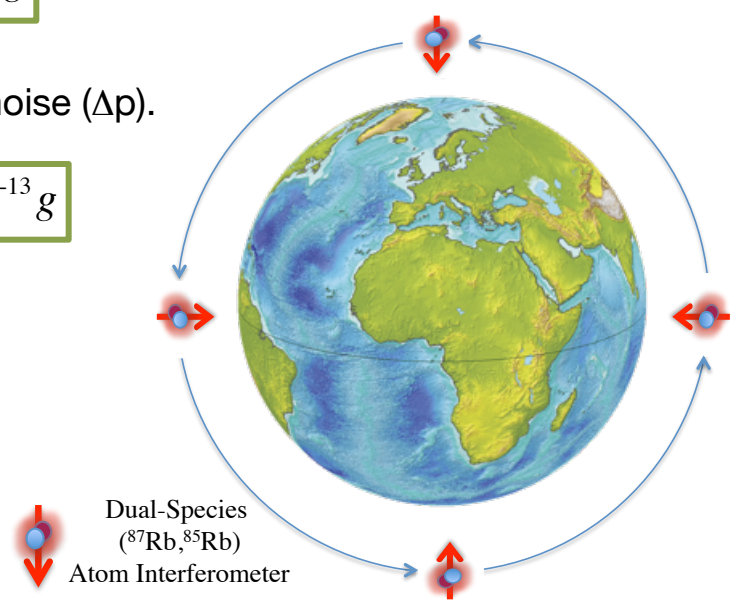

Challenges for Long-T Interferometers

Known sources that can limit the ultimate accuracy include: vibrations, rotations, accelerations, magnetic fields, differential center-of-mass position and velocity, ...

Assuming δv=1μm/s, δz=1μm, $\delta\Omega=10^{-3}\,\Omega_{ISS}$, a = 100 a_0, n_0 = 2 x 10^8/cm^3, 2T = 20s

Gravity gradient shifts

- Test masses traveling different classical paths (δr, δv) experience different gravitational potentials.

$$k_{eff}\gamma_{ZZ}(\delta z+\delta vT)T^2 = 3.0\times10^{-12}\,g$$

Rotations (centrifugal and Coriolis)

- Reduces signal contrast and systematics from different velocities.

$$-2k_{eff}\delta v_z\delta\Omega_y T^2 = 2.6\times10^{-13}\,g$$

Orders of magnitude enhanced cloud overlap necessary for WEP tests.

Mean-field shift:

- Scales with interaction strength and beam-splitter efficiency/noise (Δp).
- Fundamental density limit.

$$(4\pi\hbar a_{ij}/m)n_{j0}\Delta pT = 3.8\times10^{-13}\,g$$

Contrast loss from $\Delta\Phi$ across the cloud:

	Phase Term	$\Delta\Phi$ at T = 0.5s	T = 10s	Notes
1	$k_{eff}gT^2$	3.9×10^7	1.6×10^{10}	Gravitational
2	$2k_{eff}\cdot(\mathbf{\Omega}\times\mathbf{v})T^2$	0.9	370	Coriolis
3	$k_{eff}\gamma_{zz}(z+v_zT)T^2$	.0005	4.2	Gravity Gradient
4	$(4\pi\hbar a/m)n_0T$	.03	0.6	Mean Field Shift

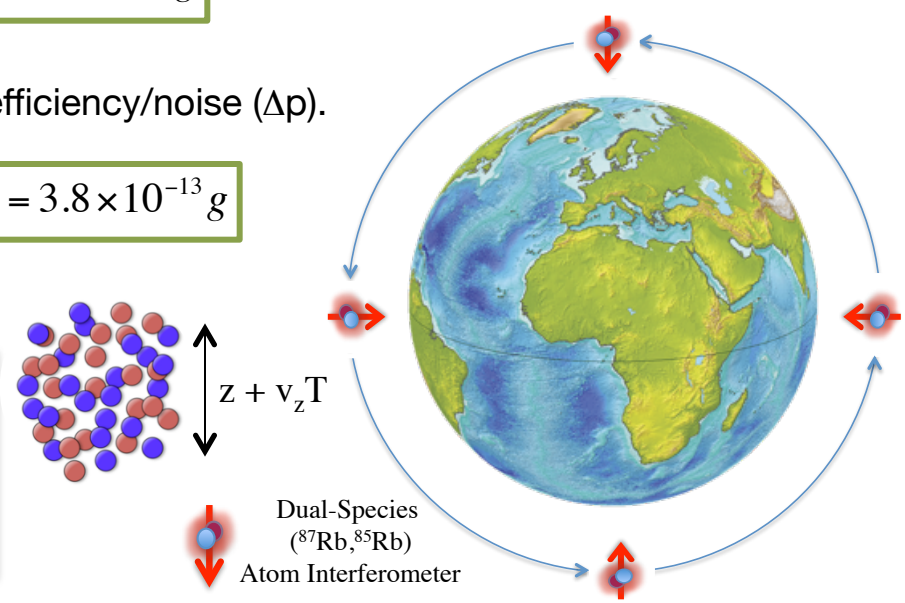

Overview

- Introduction: Precision Atom Interferometers (AI) for fundamental physics research in space.
- Study #1: *Low-energy Feshbach physics to prepare highly-overlapped dual-species atomic gases in microgravity.*
- Study #2: *Technology maturity of precision AIs for fundamental physics studies on the ISS.*

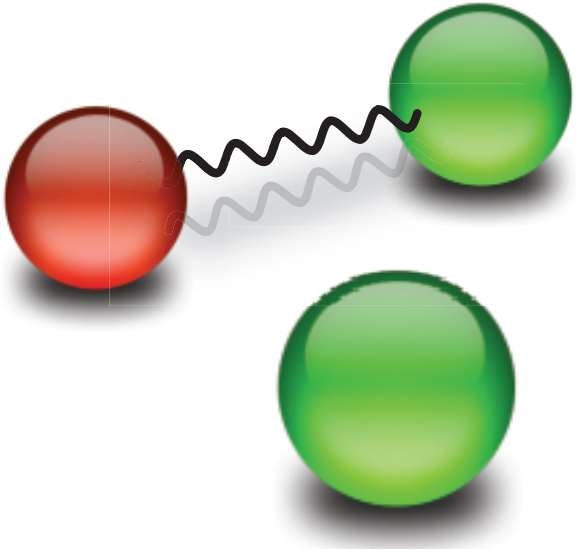

Applications of Feshbach Molecules

Fermi Gases: BEC-BCS

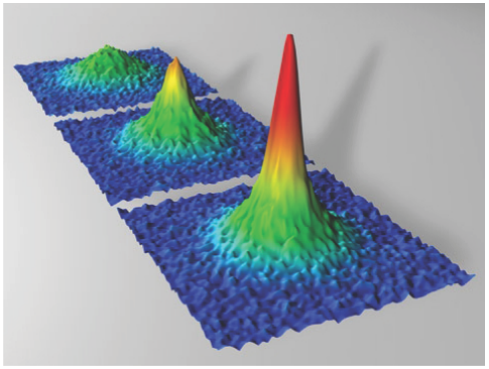

Universal Few-Body Physics

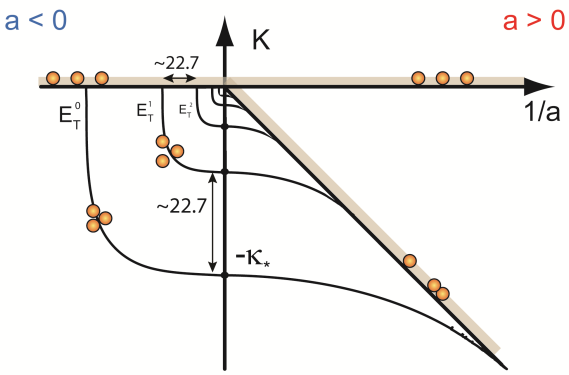

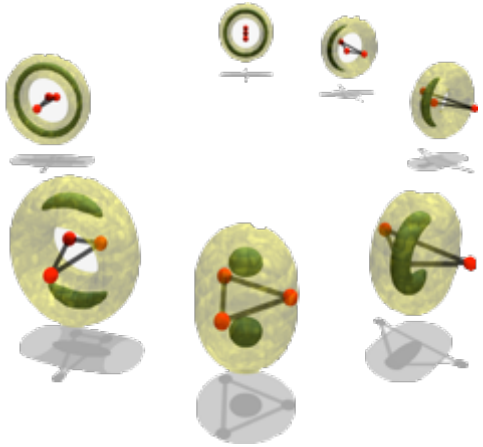

Dipolar molecules

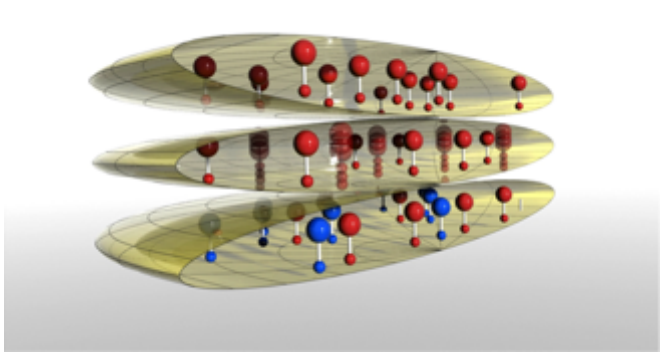

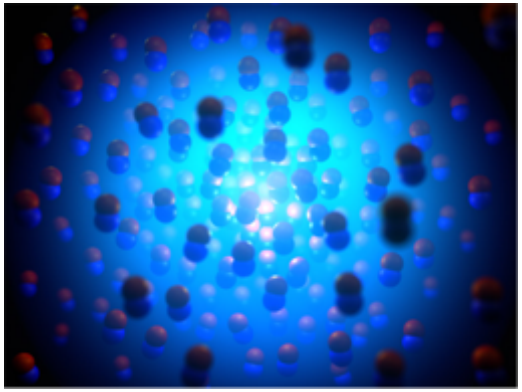

Controlled Interactions and Strongly Correlated Physics

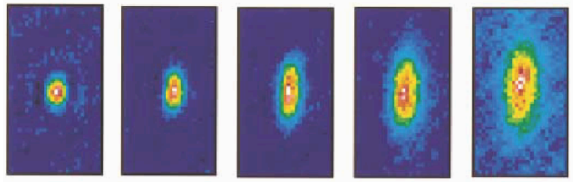

Feshbach molecules of Rb and K

Atom	ch.	ℓ	ℓ_c	B_0 (G)	Δ (G)	a_{bg}/a_0	$\delta\mu/\mu_B$	s_{res}	r_{bg}	ζ	Reference
^{39}K	*aa*	*s*	*s*	402.4	−52	−29	1.5	2.1	−0.47	0.49	D'Errico *et al.*, 2007
^{40}K	*bb*	*p*	*p*	198.4	na	na	0.134	na	na	na	Regal *et al.*, 2003b; Ticknor *et al.*, 2004[a]
	bb	*p*	*p*	198.8	na	na	0.134	na	na	na	Regal *et al.*, 2003b; Ticknor *et al.*, 2004[a]
	ab	*s*	*s*	202.1	8.0	174	1.68	2.2	2.8	3.1	Regal *et al.*, 2004[a]
	ac	*s*	*s*	224.2	9.7	174	1.68	2.7	2.8	3.8	Regal and Jin, 2003[a]
^{85}Rb	*ee*	*s*	*s*	155.04	10.7	−443	−2.33	28	−5.6	80	Claussen *et al.*, 2003
^{87}Rb	*aa*	*s*	*s*	1007.4	0.21	100	2.79	0.13	1.27	0.08	Volz *et al.*, 2003; Dürr, Volz, and Rempe, 2004[a]
	aa	*s*	*s*	911.7	0.0013	100	2.71	0.001	1.27	0.0006	Marte *et al.*, 2002[a]
	aa	*s*	*s*	685.4	0.006	100	1.34	0.006	1.27	0.004	Marte *et al.*, 2002; Dürr, Volz, and Rempe, 2004[a]
	aa	*s*	*s*	406.2	0.0004	100	2.01	0.0002	1.27	0.0001	Marte *et al.*, 2002[a]
	ae	*s*	*s*	9.13	0.015	99.8	2.00	0.008	1.27	0.005	Widera *et al.*, 2004
^{39}K ^{87}Rb	*aa*	*s*	*s*	317.9	7.6	34	2.0	0.74	0.50	0.18	Simoni *et al.*, 2008
^{40}K ^{87}Rb	*aa*	*s*	*s*	546.9	−3.10	−189	2.30	1.96	−2.75	2.70	Pashov *et al.*, 2007; Simoni *et al.*, 2008
^{41}K ^{87}Rb	*aa*	*s*	*s*	39	37	284	1.65	25.8	4.11	53.0	Simoni *et al.*, 2008; Thalhammer *et al.*, 2008
^{41}K ^{87}Rb	*aa*	*s*	*s*	79	1.2	284	1.59	0.81	4.11	1.66	Simoni *et al.*, 2008; Thalhammer *et al.*, 2008
^{85}Rb ^{87}Rb	*ec*	*s*	*s*	265.4	5.8	213					Papp and Wieman, 2006
^{85}Rb ^{87}Rb	*ec*	*s*	*s*	372	1	213					Papp and Wieman, 2006

C. Chin *et al.*, "Feshbach resonances in ultracold gases", Rev. Mod. Phys. **82**, 1225 (2010)

^{41}K – ^{87}Rb

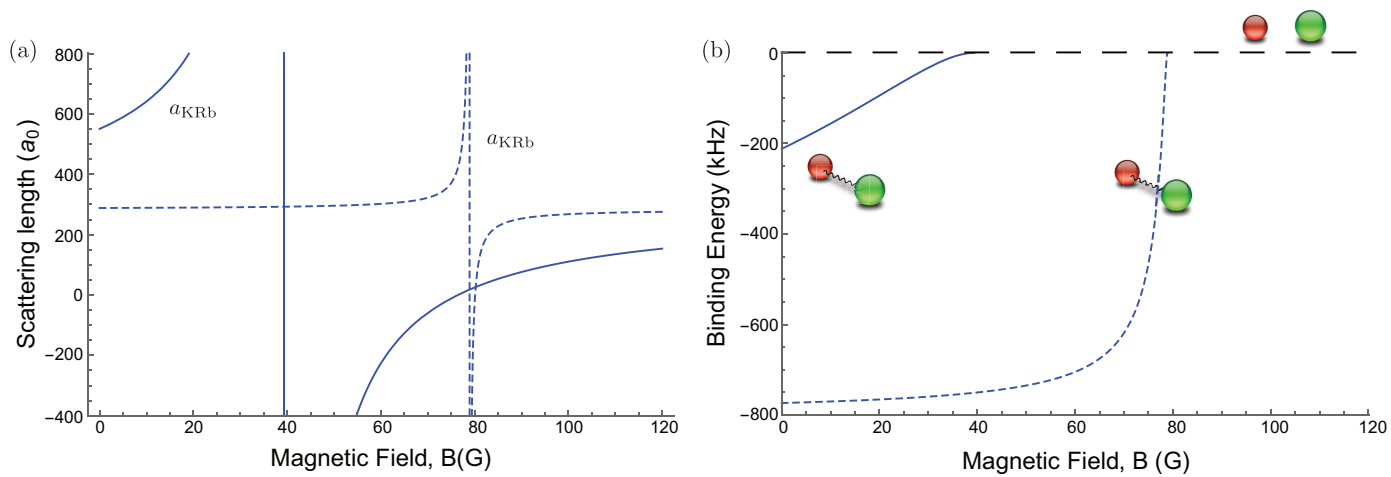

Feshbach molecules of Rb and K

Atom	ch.	ℓ	ℓ_c	B_0 (G)	Δ (G)	a_{bg}/a_0	$\delta\mu/\mu_B$	s_{res}	r_{bg}	ζ	Reference
^{39}K	*aa*	*s*	*s*	402.4	−52	−29	1.5	2.1	−0.47	0.49	D'Errico *et al.*, 2007
^{40}K	*bb*	*p*	*p*	198.4	na	na	0.134	na	na	na	Regal *et al.*, 2003b; Ticknor *et al.*, 2004[a]
	bb	*p*	*p*	198.8	na	na	0.134	na	na	na	Regal *et al.*, 2003b; Ticknor *et al.*, 2004[a]
	ab	*s*	*s*	202.1	8.0	174	1.68	2.2	2.8	3.1	Regal *et al.*, 2004[a]
	ac	*s*	*s*	224.2	9.7	174	1.68	2.7	2.8	3.8	Regal and Jin, 2003[a]
^{85}Rb	*ee*	*s*	*s*	155.04	10.7	−443	−2.33	28	−5.6	80	Claussen *et al.*, 2003
^{87}Rb	*aa*	*s*	*s*	1007.4	0.21	100	2.79	0.13	1.27	0.08	Volz *et al.*, 2003; Dürr, Volz, and Rempe, 2004[a]
	aa	*s*	*s*	911.7	0.0013	100	2.71	0.001	1.27	0.0006	Marte *et al.*, 2002[a]
	aa	*s*	*s*	685.4	0.006	100	1.34	0.006	1.27	0.004	Marte *et al.*, 2002; Dürr, Volz, and Rempe, 2004[a]
	aa	*s*	*s*	406.2	0.0004	100	2.01	0.0002	1.27	0.0001	Marte *et al.*, 2002[a]
	ae	*s*	*s*	9.13	0.015	99.8	2.00	0.008	1.27	0.005	Widera *et al.*, 2004
^{39}K ^{87}Rb	*aa*	*s*	*s*	317.9	7.6	34	2.0	0.74	0.50	0.18	Simoni *et al.*, 2008
^{40}K ^{87}Rb	*aa*	*s*	*s*	546.9	−3.10	−189	2.30	1.96	−2.75	2.70	Pashov *et al.*, 2007; Simoni *et al.*, 2008
^{41}K ^{87}Rb	*aa*	*s*	*s*	39	37	284	1.65	25.8	4.11	53.0	Simoni *et al.*, 2008; Thalhammer *et al.*, 2008
^{41}K ^{87}Rb	*aa*	*s*	*s*	79	1.2	284	1.59	0.81	4.11	1.66	Simoni *et al.*, 2008; Thalhammer *et al.*, 2008
^{85}Rb ^{87}Rb	*ec*	*s*	*s*	265.4	5.8	213					Papp and Wieman, 2006
^{85}Rb ^{87}Rb	*ec*	*s*	*s*	372	1	213					Papp and Wieman, 2006

C. Chin *et al.*, "Feshbach resonances in ultracold gases", Rev. Mod. Phys. **82**, 1225 (2010)

^{41}K – ^{87}Rb

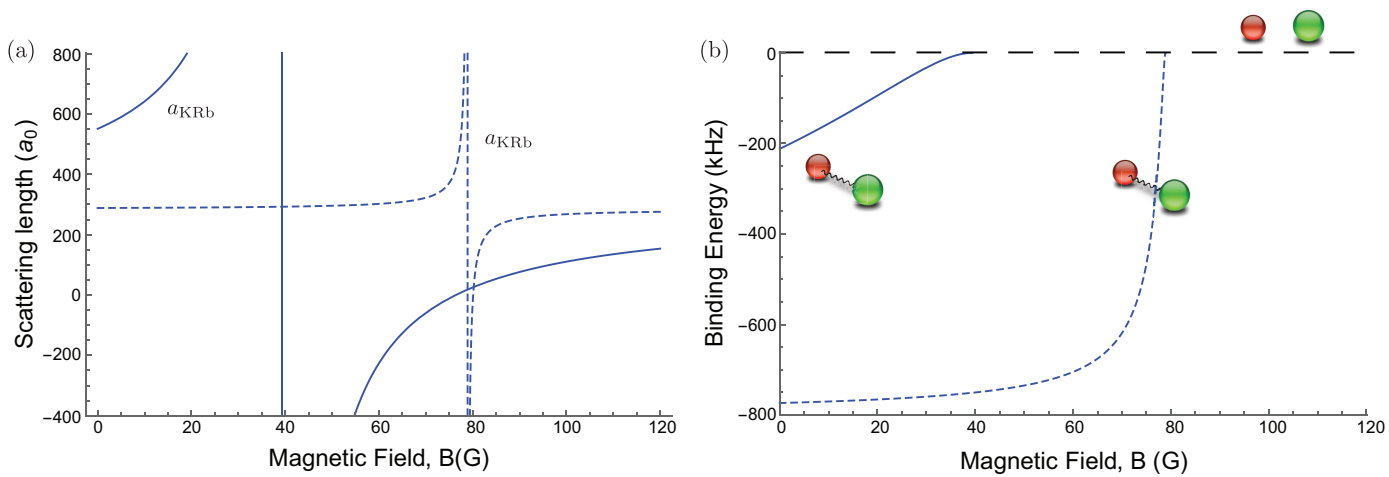

Feshbach molecules of Rb and K

Universality

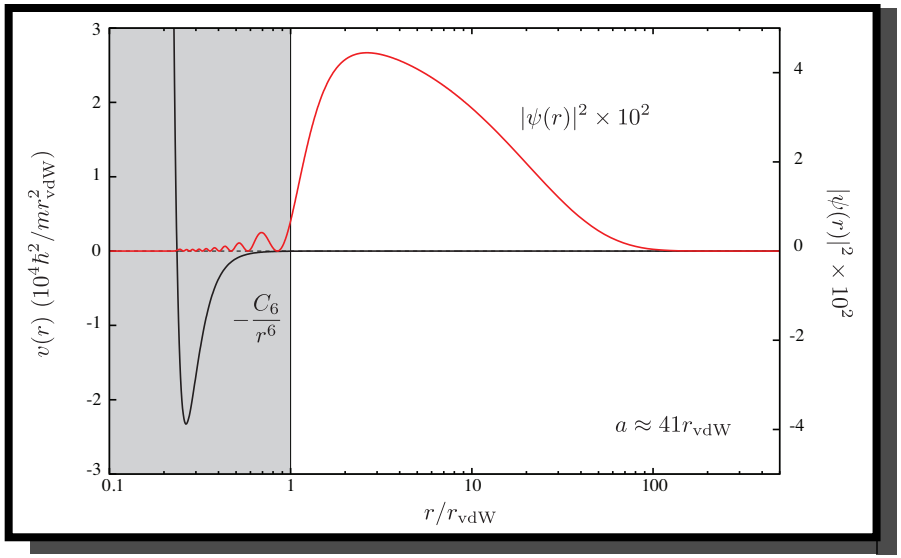

Dimer Size: $\langle r \rangle = a/2$

Binding Energy: $E_D \approx \frac{-\hbar^2}{ma^2}$

$^{41}K - ^{87}Rb$

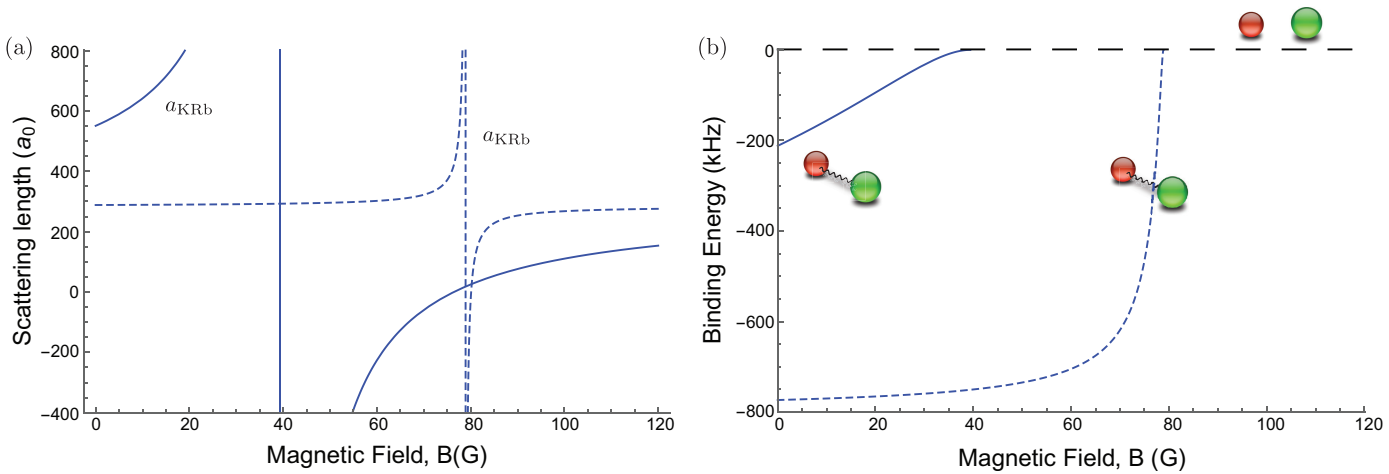

CAL NRA in a Nutshell

#1:

Low-energy Feshbach physics to prepare highly-overlapped dual-species atomic gases in microgravity

- Negate systematics scaling with dr and dv.
- Molecular state-control at k_B*1 nK.

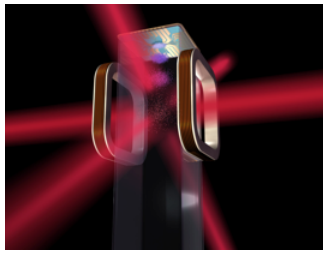

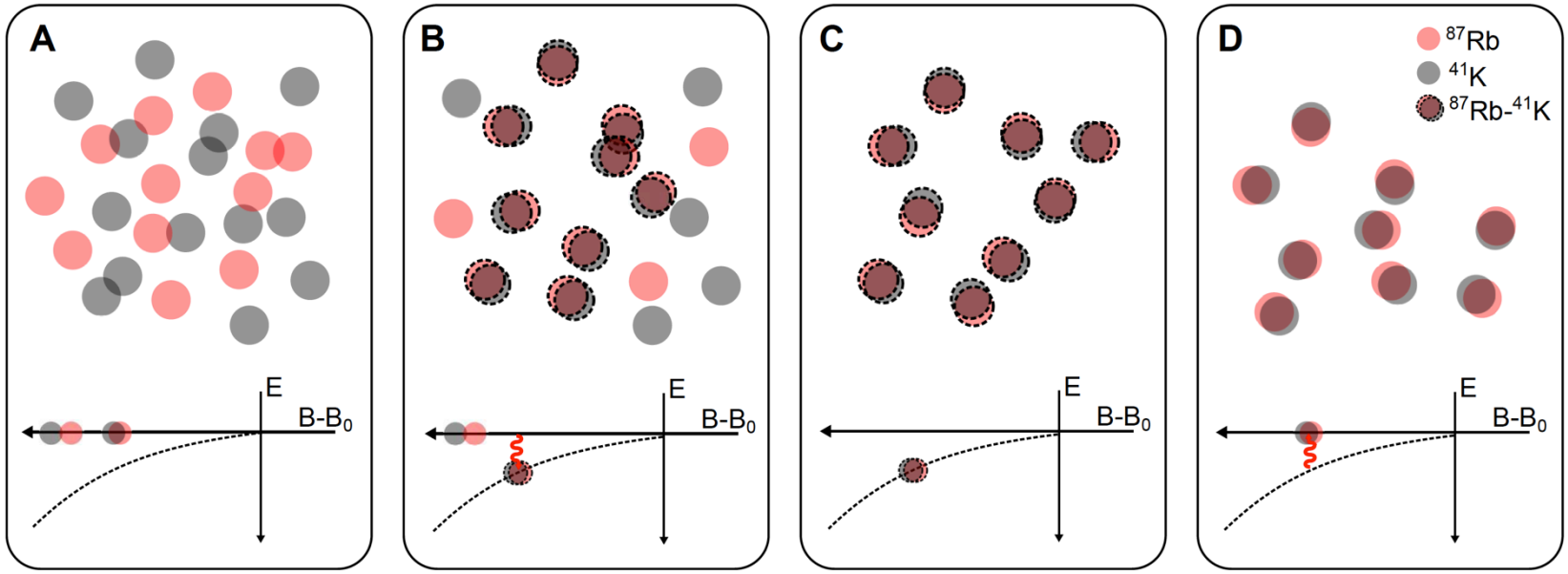

- (A) Start with ^{41}K-^{87}Rb dual species gases co-trapped and cooled to ~ 1 nK.
- (B + C) Heteronuclear Feshbach molecule formation (RF) and filtering out free atoms
- (D) Molecular dissociation w/Fourier-limited heating and negligible loss.

Technical Considerations for Study #1

Explore Feshbach physics in microgravity and it's potential as a preparation tool for mitigating systematics in high-precision dual-species AI requires:

- **Sufficient preparation** of heteronuclear gases.
  - Ultra-low temperature
  - Long lifetime
  - Negligible heating
- **Sufficient control** of external forces/perturbations.
  - Magnetic fields and gradients, stray light, vibrations ...
- **Sufficient detection** to measure overlap.

Atomic and Molecular Losses

Three-body Recombination

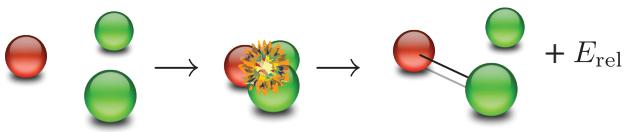

System	s_0	C_3	C_β	$a_0(\mathrm{a}_0)$	$a_*(\mathrm{a}_0)$	η
^{87}Rb^{87}Rb^{41}K	0.644	340.1	10.3	2800	230	0.12
^{87}Rb^{41}K^{41}K	0.246	139.3	22.9	7000	—	0.02

Helfrich et al., PRA (2010); Wang et al., PRL (2012);
Bloom et al., PRL (2013); Barontini et al., PRL (2009)

$$L_3 = \frac{L_3^0}{1 + L_3^0/L_3^u}, \qquad L_3^u = \frac{32\pi^2}{\mu}\frac{1-e^{-4\eta}}{(2\mu T)^2},$$

$$L_3^0 = C_3 \frac{\sin^2(s_0 \ln \frac{a}{a_0}) + \sinh^2\eta}{\sinh^2(\pi s_0 + \eta) + \cos^2(s_0 \ln \frac{a}{a_0})}\frac{a^4}{m_X},$$

D'Incao et al., PRL (2004); Helfrich et al., PRA (2010);

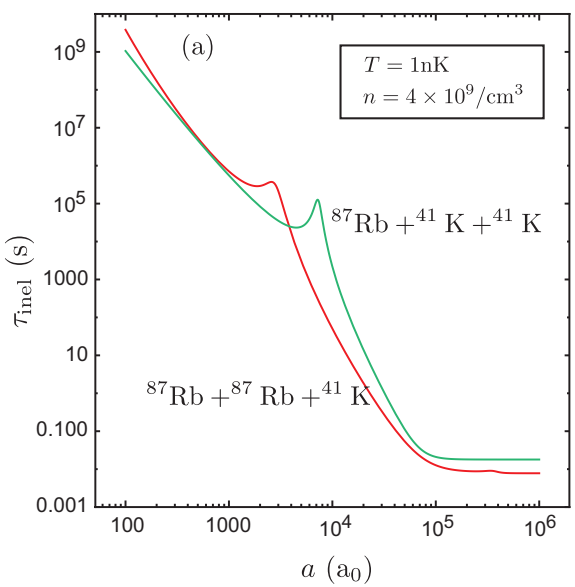

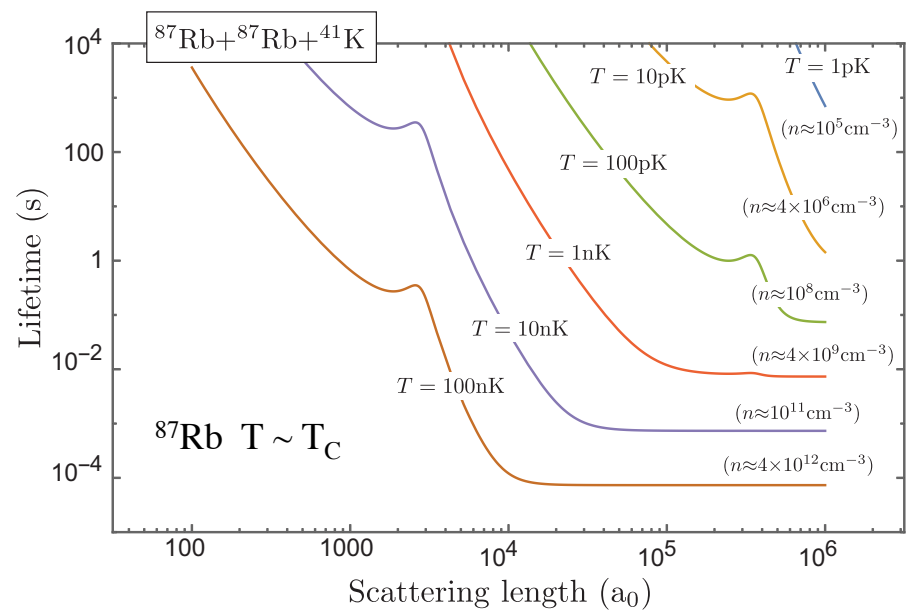

Atomic and Molecular Losses

Atom-diatom inelastic collisions

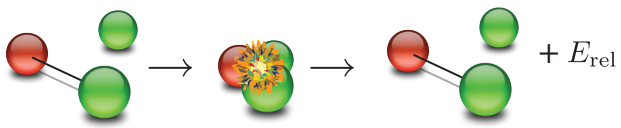

System	s_0	C_3	C_β	$a_0(\mathrm{a}_0)$	$a_*(\mathrm{a}_0)$	η
^{87}Rb^{87}Rb^{41}K	0.644	340.1	10.3	2800	230	0.12
^{87}Rb^{41}K^{41}K	0.246	139.3	22.9	7000	—	0.02

Helfrich et al., PRA (2010); Wang et al., PRL (2012);
Bloom et al., PRL (2013); Barontini et al., PRL (2009)

$$\boxed{\beta = \frac{\beta^0}{1+\beta^0/\beta^u},} \qquad \beta^u = \frac{2\pi^{1/2}}{\mu_{ad}}\frac{1-e^{-4\eta}}{(2\mu_{ad}T)^{1/2}},$$

$$\beta^0 = C_\beta \frac{\sinh 2\eta}{\sin^2(s_0 \ln \frac{a}{a_*}) + \sinh^2\eta}\frac{a}{m_X},$$

D'Incao et al., PRL (2004); Helfrich et al., PRA (2010);

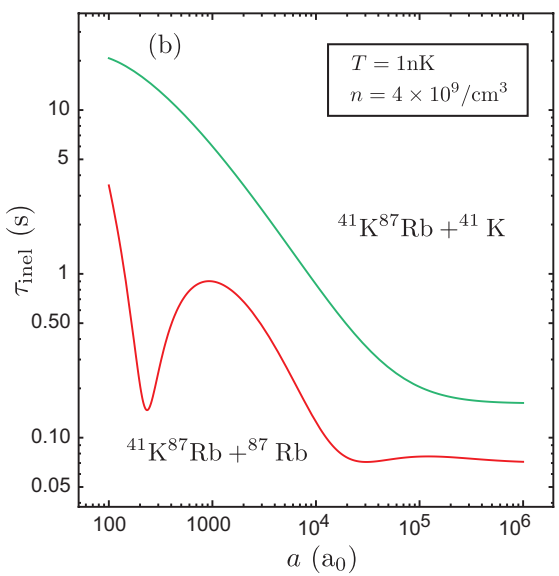

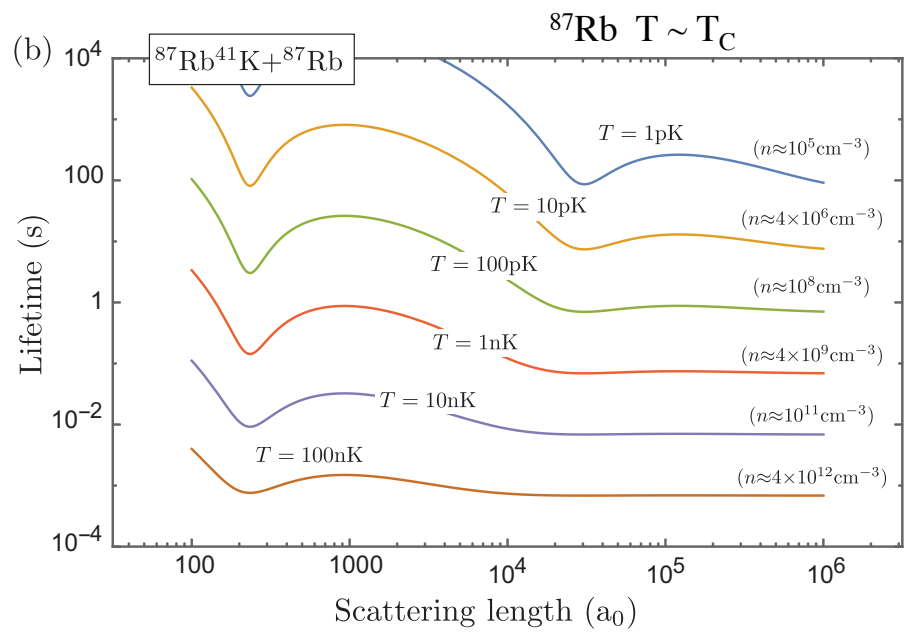

Molecular Association/Dissociation

Feshbach Molecule Association

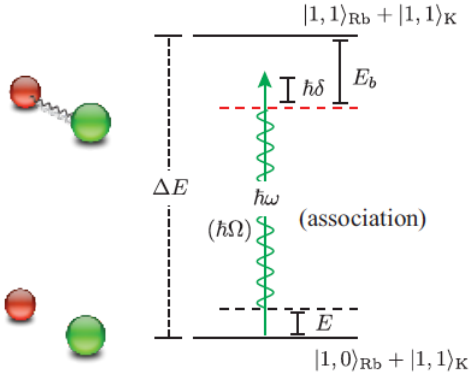

Association probability:

$$P_m(E,\tau) \;=\; e^{-\gamma t/2}\left(\frac{\Omega_m}{\Omega_{\rm eff}^m}\right)^2 \left|\sin\left(e^{i\theta_m}\frac{\Omega_{\rm eff}^m \tau}{2}\right)\right|^2,$$

(Association under ground conditions)

$$(T = 200\text{nK},\; n = 5\times 10^{11}/\text{cm}^3)$$

$T = 200\text{nK},\;\; \Omega_m \approx 1.2\text{kHz},\;\; \gamma = 70\text{Hz}$
$(k_B T/\hbar\Omega_m \approx 3.5,\;\; \pi\gamma/2\Omega_m \approx 0.02)$

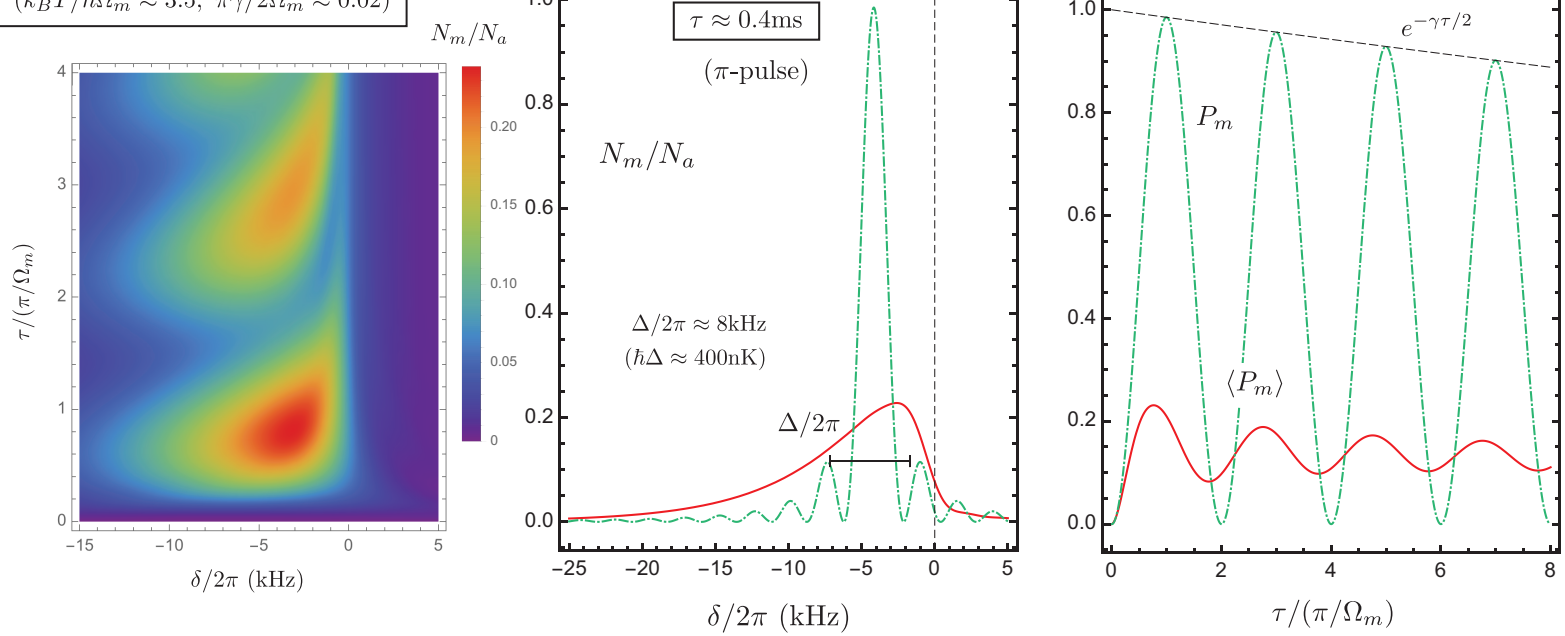

Molecular Association/Dissociation

Feshbach Molecule Association

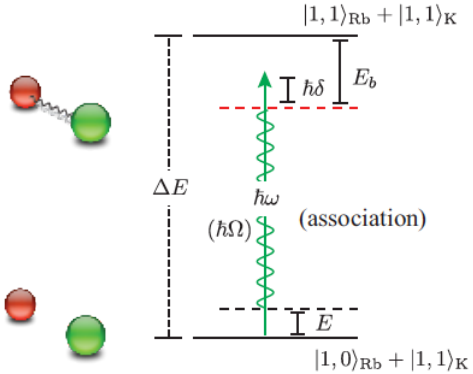

$T = 1\text{nK},\ \Omega_m \approx 34.9\text{Hz},\ \gamma = 2.4\,\text{Hz}$
$(k_B T/\hbar\Omega_m \approx 0.60, \pi\gamma/2\Omega_m \approx 0.02)$

Association probability:

$$P_m(E,\tau) = e^{-\gamma t/2}\left(\frac{\Omega_m}{\Omega_{\rm eff}^m}\right)^2 \left|\sin\left(e^{i\theta_m}\frac{\Omega_{\rm eff}^m \tau}{2}\right)\right|^2,$$

(Association under CAL conditions)

$$(T = 1\text{nK},\ n = 4\times 10^9/\text{cm}^3)$$

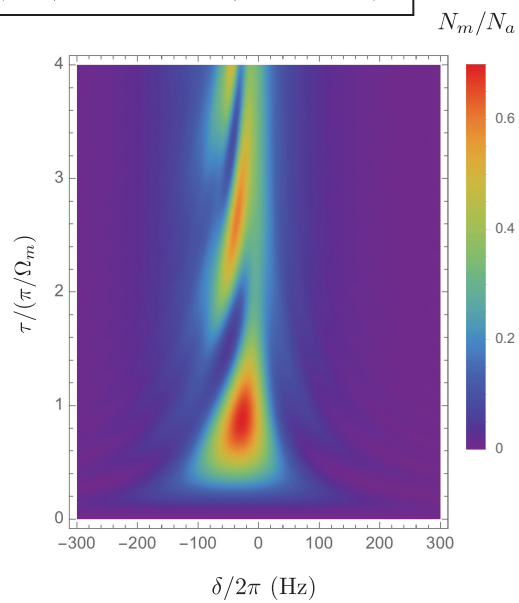

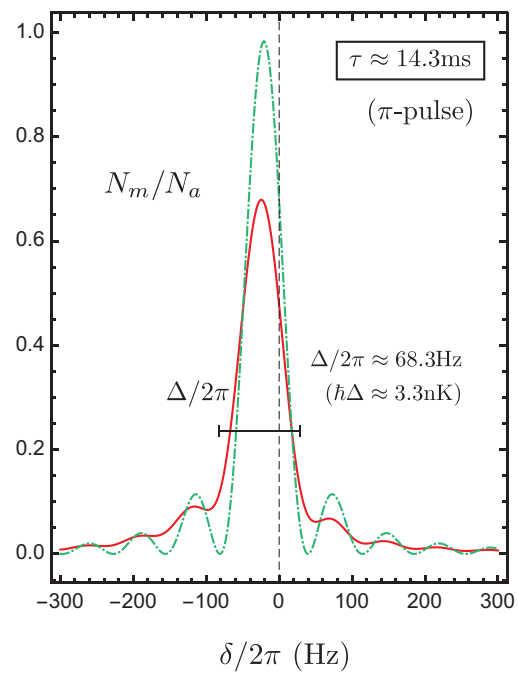

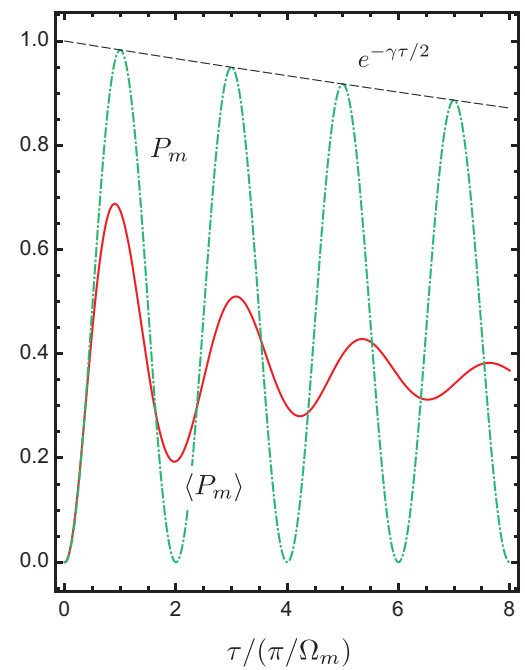

Molecular Association/Dissociation

Feshbach Molecule Dissociation

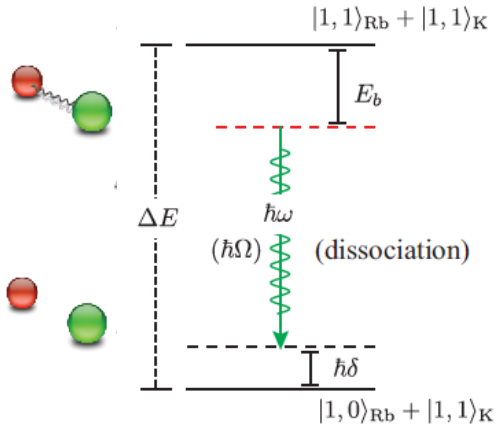

Dissociation probability:

$$P_K(\hbar\delta, t) = e^{-\gamma t/2}\left(\frac{\Omega_m}{\Omega_{\rm eff}^K}\right)^2 \left|\sin\left(e^{i\theta_K}\frac{\Omega_{\rm eff}^K t}{2}\right)\right|^2,$$

(Dissociation under CAL conditions)

$$(T = 1\text{nK},\ n = 4\times 10^9/\text{cm}^3)$$

$$p_1 = -p_2 = \sqrt{m_i\hbar\delta}$$

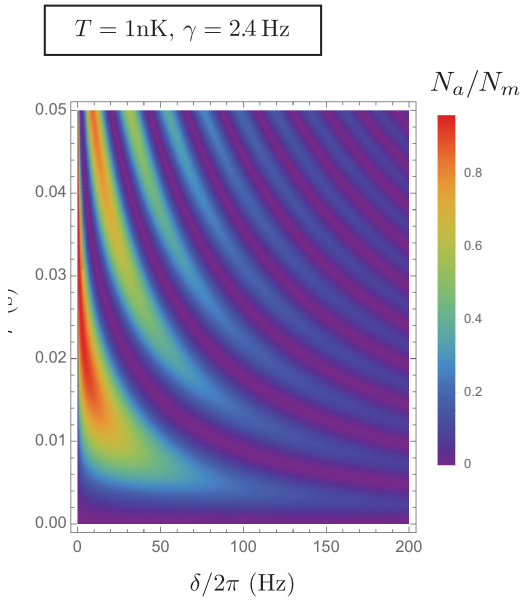

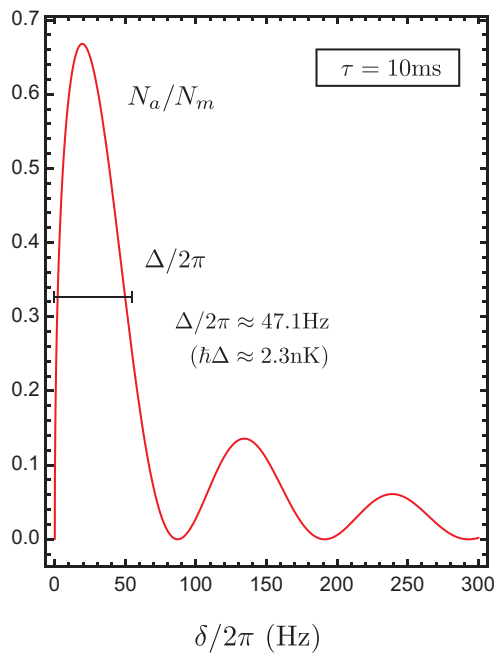

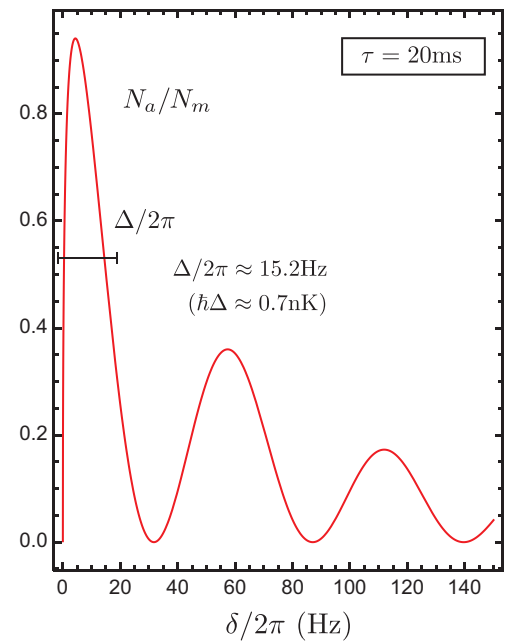

Microgravity Justification

- Extrapolating measurements of ^{87}Rb-^{41}K dimers* to CAL
  ➔ long-lived, ultra-low-energy molecules in freefall.

	T_C (nK)	E_M	Molecule #	n_0 (atoms/cm^3)	Lifetime
LENS*	200	40%	1.2×10^4	5×10^{11}	60μs – 5ms
NASA/CAL	1	70%	$> 10^4$	4×10^9	> 100ms

BEC condensate temperature (T_c), Feshbach molecule conversion efficiency (E_M), total molecule number, peak single-atom densities (n_0) and Feshbach molecule lifetime (τ) comparisons between the realized ^{41}K^{87}Rb ultracold gas at LENS and the corresponding parameters expected for these dual-species gases on the NASA/CAL facility.

* C. Weber *et al.*, "Association of ultracold double-species bosonic molecules" Phys. Rev. A, **78**, 061601 (2008)

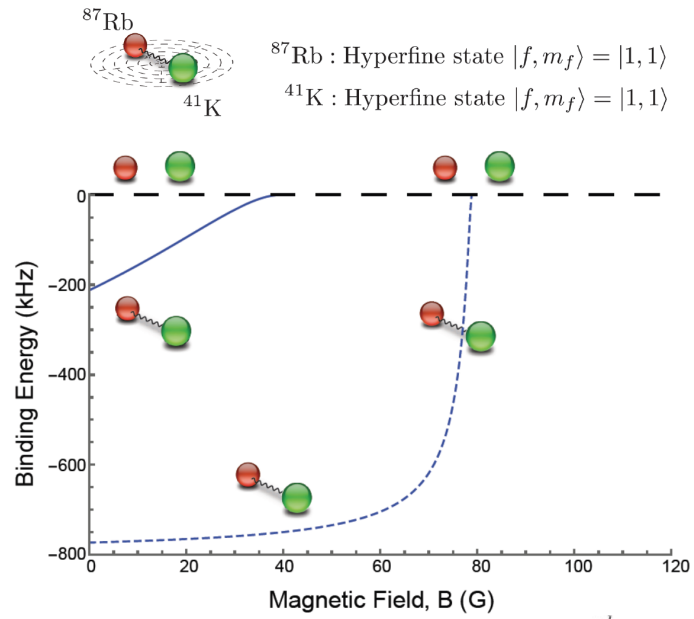

- Gravitational sag (reduced cloud overlap):
  - Requires stronger confinement -> higher T, n_0
  - High A-D and D-D loss rates (τ^{-1}).
  - Constrained by thermal energy (few 100s nK).

- On the ISS (microgravity):
  - Unconfined gases, n_0 and T reduced by ~ 10^3
  - Molecule lifetime increased to ~ 1s
  - Kinetic energy (few 100s pK) unexplored for FR physics

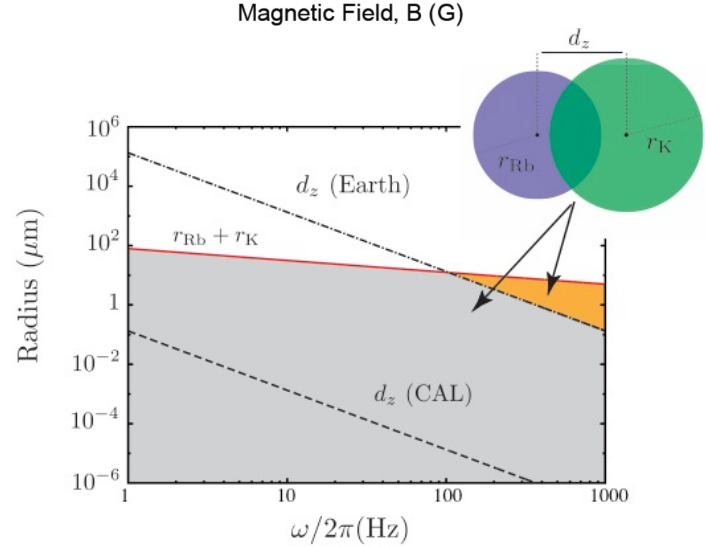

Parameters: $a_{\rm Rb} = 100a_0$, $a_{\rm K} = 60a_0$, $N_{\rm Rb} = 2 \times 10^5$, $N_{\rm K} = 3 \times 10^4$

Error Budget

Preliminary Error Budget for ^{87}Rb and ^{41}K CM overlap

	Systematic	CM position	CM velocity	Comments
1	1st Order Zeeman	0.17nm	34nm/s	Mitigated by dissociating ^{41}K and ^{87}Rb to the clock states.
2	2nd Order Zeeman	$<$ 0.1nm	2nm/s	Independent of B-field magnitude by field-direction modulation.
3	RF Photon	$<$ 5pm	$<$ 0.5nm/s	Recoil from 35 MHz RF pulse at dissociation.
4	Vibrations	$<$ 4nm		Camera movement over 1 ms assuming $S(g) < 3 \times 10^{-7} g^2/Hz$.
5	Gravity	$<$ 50pm		Assuming 10 μg residual acceleration and 1 ms imaging delay between species.
6	Imaging Light	$<$ 1pm		Off-resonant scattering of ^{41}K atoms during imaging pulse for ^{87}Rb.
	Total	**$<$ 5 nm**	**$<$ 35 nm/s**	

Assuming B = 1 Gauss and ΔB = 10 mGauss/cm, detection 10ms after dissociation, RF spectroscopy and Stern-Gerlach separation to characterize fields to a part in 10^3.

Magnetic Field Error Budget

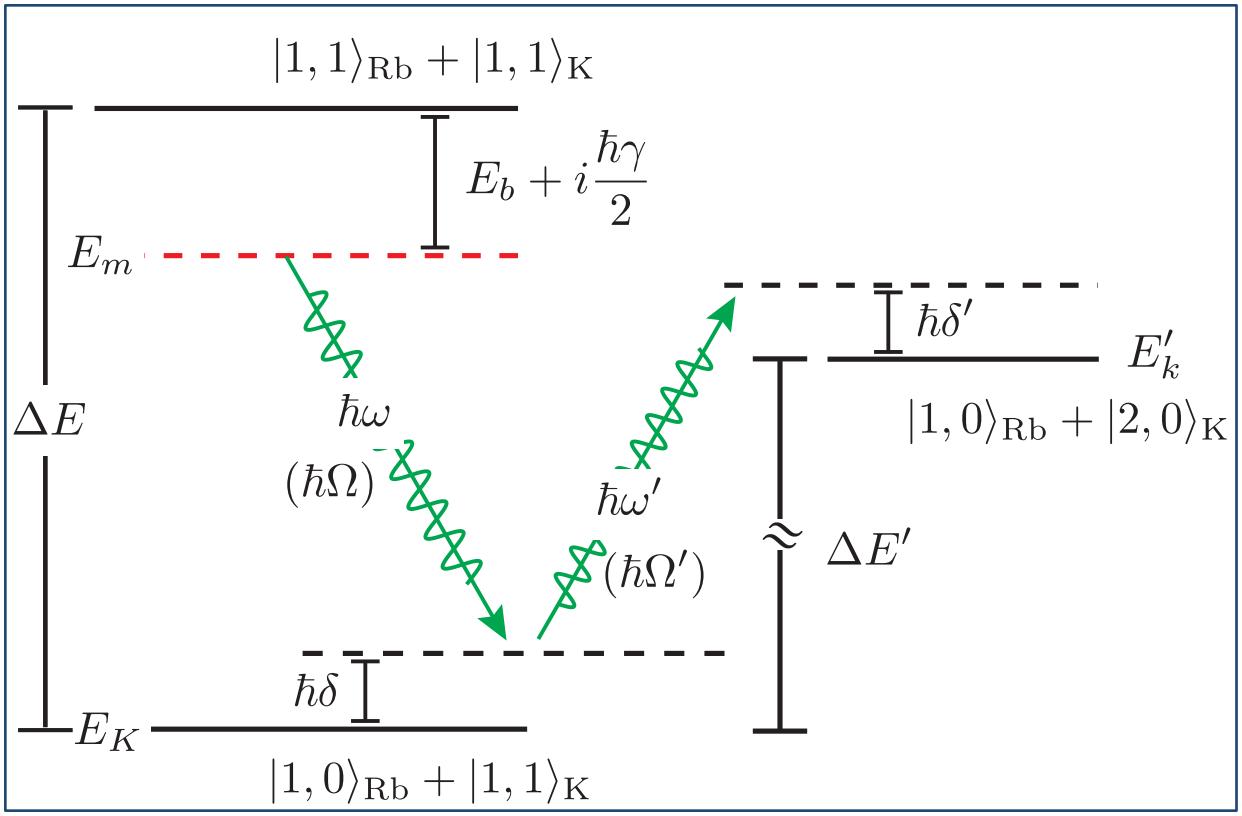

- Explore two-photon RF (^{87}Rb) + microwave (^{41}K) dissociation to eliminate systematics from 1st Order shifts.

$$^{41}K|1,1\rangle +^{87} Rb|1,1\rangle \rightarrow^{41} K|2,0\rangle +^{87} Rb|1,0\rangle$$

Error Budget

Preliminary Error Budget for ^{87}Rb and ^{41}K CM overlap

	Systematic	CM position	CM velocity	Comments
1	1st Order Zeeman	0.17nm	34nm/s	Mitigated by dissociating ^{41}K and ^{87}Rb to the clock states.
2	2nd Order Zeeman	$<$ 0.1nm	2nm/s	Independent of B-field magnitude by field-direction modulation.
3	RF Photon	$<$ 5pm	$<$ 0.5nm/s	Recoil from 35 MHz RF pulse at dissociation.
4	Vibrations	$<$ 4nm		Camera movement over 1 ms assuming $S(g) < 3 \times 10^{-7} g^2/Hz$.
5	Gravity	$<$ 50pm		Assuming 10 μg residual acceleration and 1 ms imaging delay between species.
6	Imaging Light	$<$ 1pm		Off-resonant scattering of ^{41}K atoms during imaging pulse for ^{87}Rb.
	Total	**$<$ 5 nm**	**$<$3 nm/s**	

Assuming B = 1 Gauss and ΔB = 10 mGauss/cm, detection 10ms after dissociation, RF spectroscopy and Stern-Gerlach separation to characterize fields to a part in 10^3.

Overview

- Introduction: Precision Atom Interferometers (AI) for fundamental physics research in space.
- Study #1: *Low-energy Feshbach physics to prepare highly-overlapped dual-species atomic gases in microgravity.*
- Study #2: *Technology maturity of precision AIs for fundamental physics studies on the ISS.*

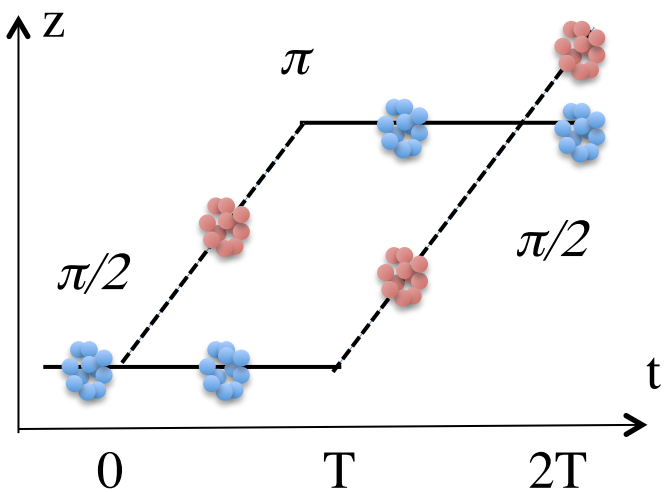

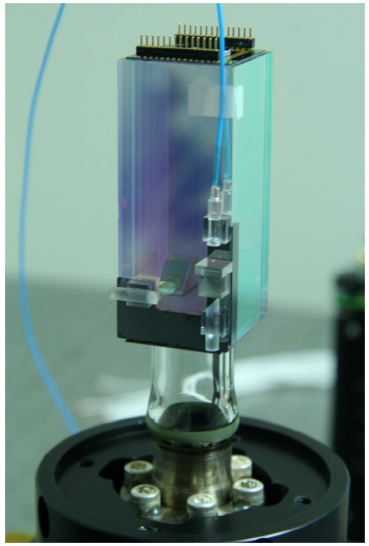

Atom Interferometer Experiments Onboard the ISS

Spatially constrained AI

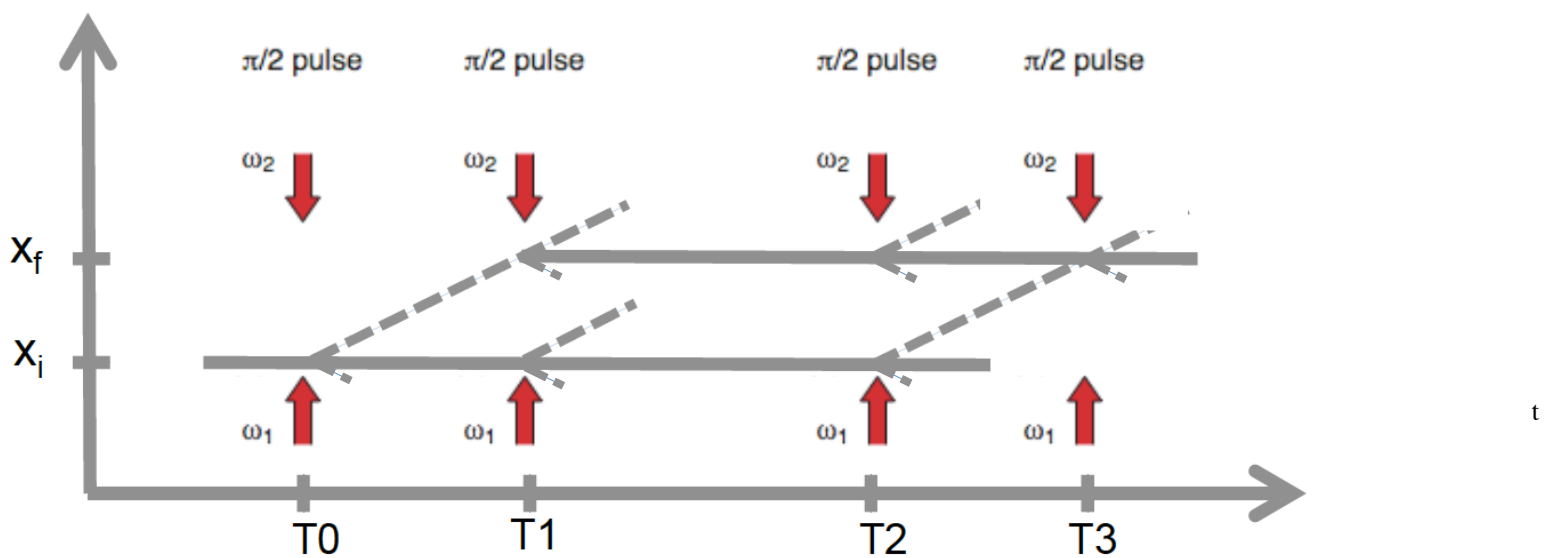

Demonstrate AI atom-photon coherence beyond ~ 2 seconds* for ^{87}Rb.

- Constrained Bragg beam path length (~2”) and imaging region (~10mm) on CAL prohibit MZ AI with $2T > 1.5$ s.
- Implement “spatially constrained AI” topology, limited by contrast and thermal expansion (~100 microns per second at 100 pK), sufficient for > 3s free fall.

*Current record is 2T = 2.3s by S. Dickerson *et al.*, “Multiaxis Inertial Sensing with Long-Time Point Source Atom Interferometry” PRL, **111**, 083001(2013)

Atom Interferometer Experiments Onboard the ISS

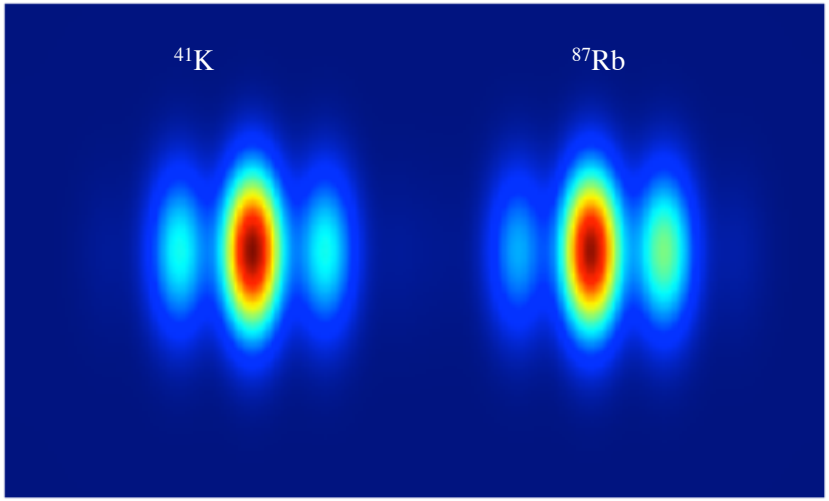

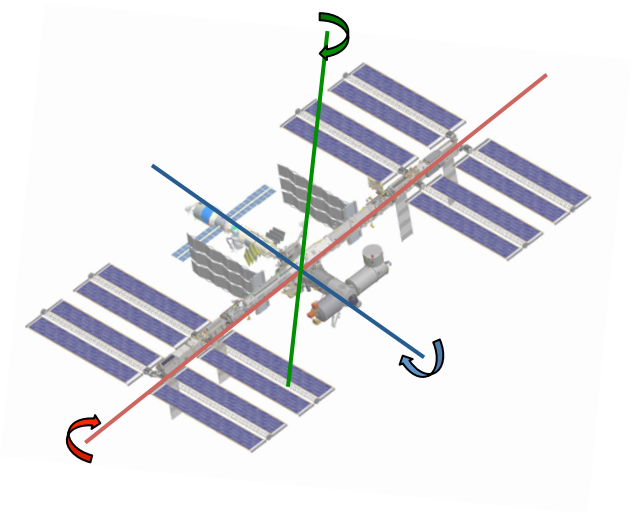

ISS rotation noise measurement from AI-induced phase fringes.

- For $2T$ = 1s, 1nK ^{87}Rb cloud (σ_v is the thermal Gaussian width), and $\Omega = \Omega_{ISS} = 2\pi/91$min:

$$2k_{eff}(\Omega \times \sigma_v)T^2 = 3.6rad$$

- Observation of fringes in each shot from rotation of CAL Physics Package on ISS.

ISS Rotation Noise Measurements

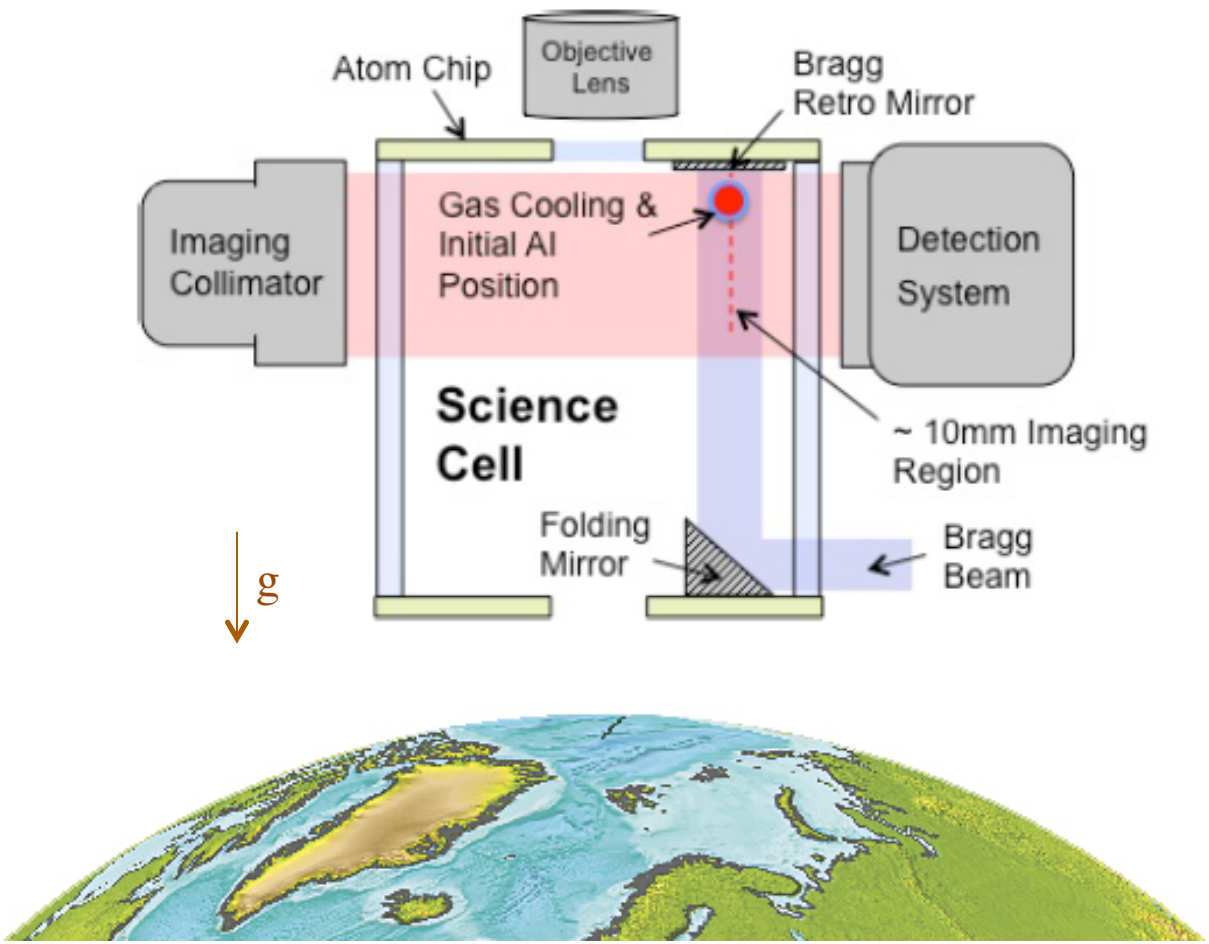

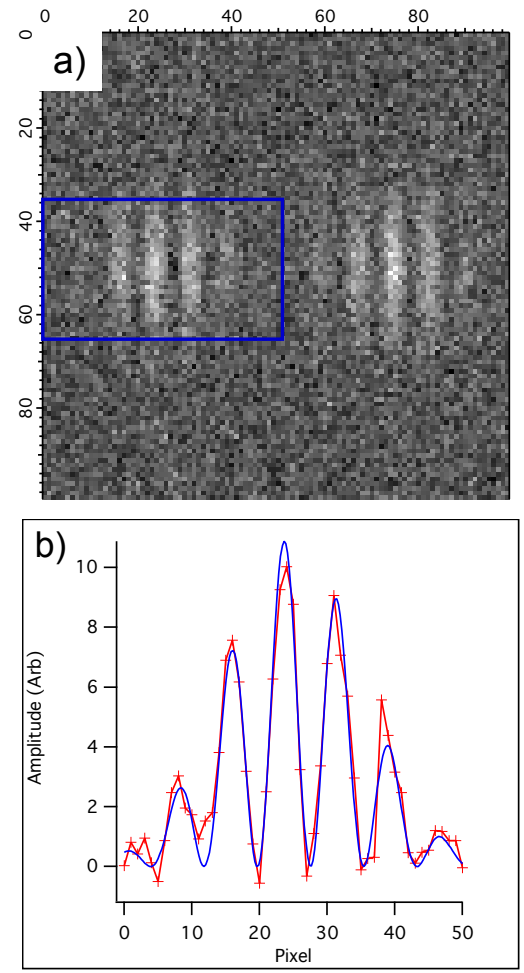

(Top) Simulated fringe pattern on single-shot ^{87}Rb 2D density profile from DC angular velocity of the ISS with T = 0.5s AI and $N_{87} = 10^5$. (Bottom) Line profile after vertically averaging and fit (blue) to extract fringe spacing to a part in 10^2.

Velocity of station is into the page.
This is the ideal orientation for imaging fringes

Overview

- Introduction: Precision Atom Interferometers (AI) for fundamental physics research in space.
- Study #1: *Low-energy Feshbach physics to prepare highly-overlapped dual-species atomic gases in microgravity.*
- Study #2: *Technology maturity of precision AIs for fundamental physics studies on the ISS.*
- *Potential follow on studies*

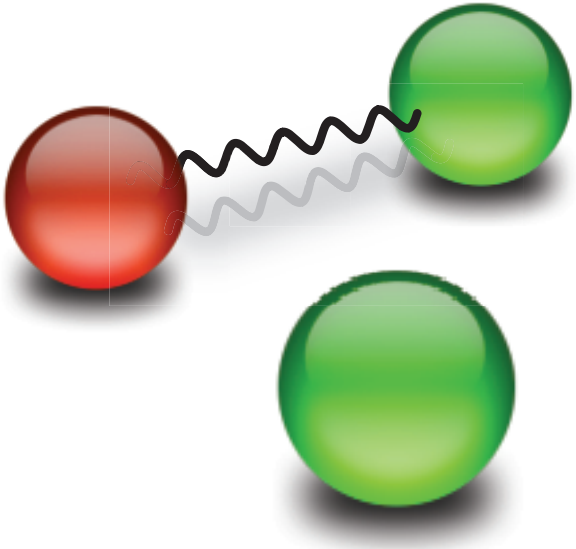

Potential Follow-On Studies

Follow-on investigations of the dual-species Feshbach molecule studies:

- Feshbach physics may provide a simplification/enhancement of dual-species DKC

Delta kick cooling:

1) Evaporative cooling and release of the gas from a harmonic potential for a time t_f.

2) Brief pulse of potential for time t_k minimizes velocity distribution when:

$$t_k * t_f = 1/\omega^2$$

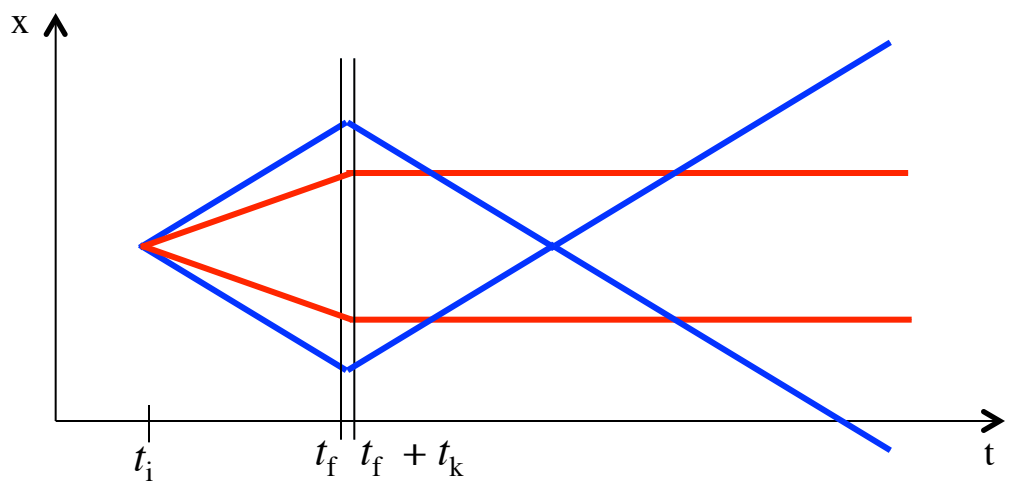

Mass dependence of the trapping potential:
$\omega_1^2 / \omega_2^2 = m_2 / m_1$ makes dual-species DKC difficult.

Long-lived Feshbach molecules may be used to efficiently cool two atomic species simultaneously with the simplicity of single-pulse DCK.

Potential Follow-On Studies

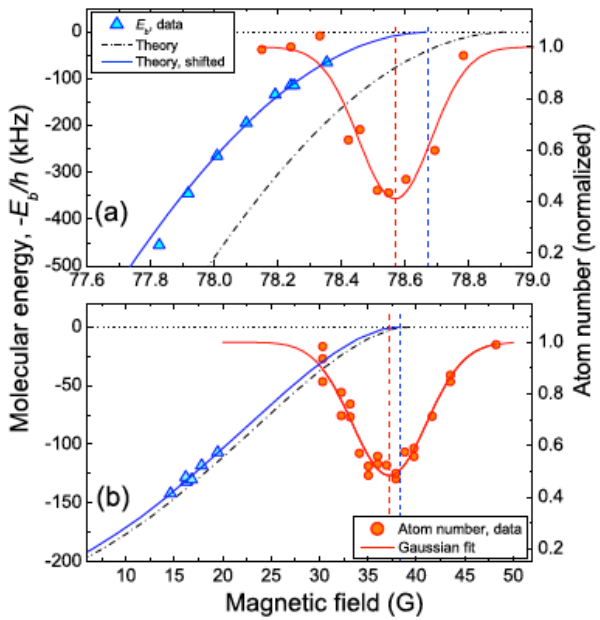

Enhanced Sensitivity on β near FR

- In cold collisions, the scattering phase shift is very sensitive to changes of the electron-proton mass ratio :

$$\phi \sim (V/m_{at})^{1/2} \sim (m_e/m_p)^{1/2} = \beta^{1/2}$$

- Near narrow Feshbach resonances, enhancement of the scattering length gives

$$\Delta a/a = K\, \delta\beta/\beta$$

where K can be as large as $10^9 - 10^{12}$.

Current best estimate of time-variation of β:

$$\Delta\beta/\beta < 2 \times 10^{-17}/\text{yr}$$

with knowledge of δ**a/a** to 10^{-6}, can expect in one year:

$$\Delta\beta/\beta < 10^{-15} - 10^{-18}/\text{yr}$$

- C. Chin et al. *Ultracold molecules: new probes on the variation of fundamental constants*, New Journal of Physics **11**, 055048 (2009)
- M. Gacesa and R. Côté *Photoassociation of ultracold molecules near a Feshbach resonance as a probe of the electron-proton mass ratio*, Journal of Molecular Spectroscopy **300**, 124 (2014)

Potential Follow-On Studies

Follow-on investigations derived from the dual-species Feshbach molecule studies:

- Test quantum wave nature of large s-wave "halo" molecules $\langle r \rangle > 500$ nm for $a > 10{,}000\ a_0$
- Scattering of quantum particles with internal structure from a slit. (*Quantum Ulm sparrow*)

B. Shore *et al*. (2015) *New J. Phys*. **17**, 013046

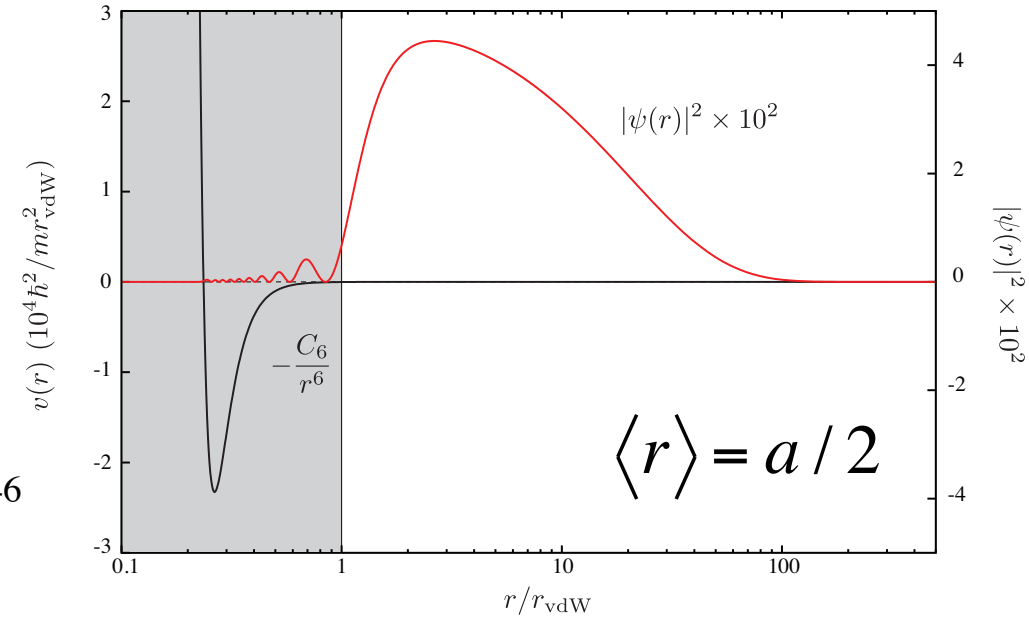

Matter-wave interferometry mass record: 810 atoms, diameter ~ 3nn.

KDTLI Interferometer

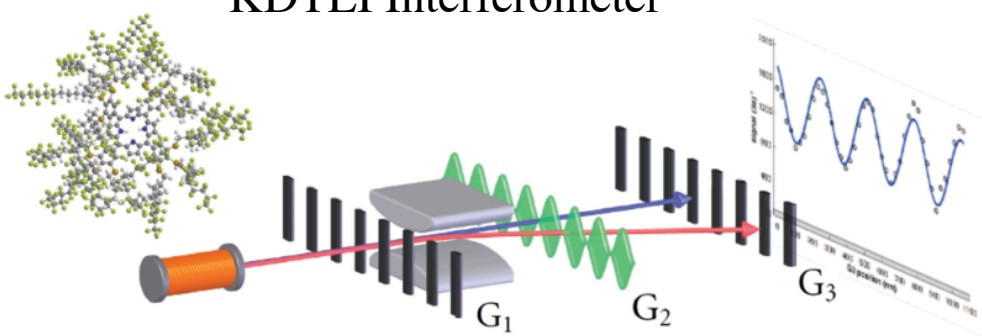

S. Eidenburger *et al*. (2013) *Phys. Chem. Chem. Phys*. **15**, 14656

Contributors

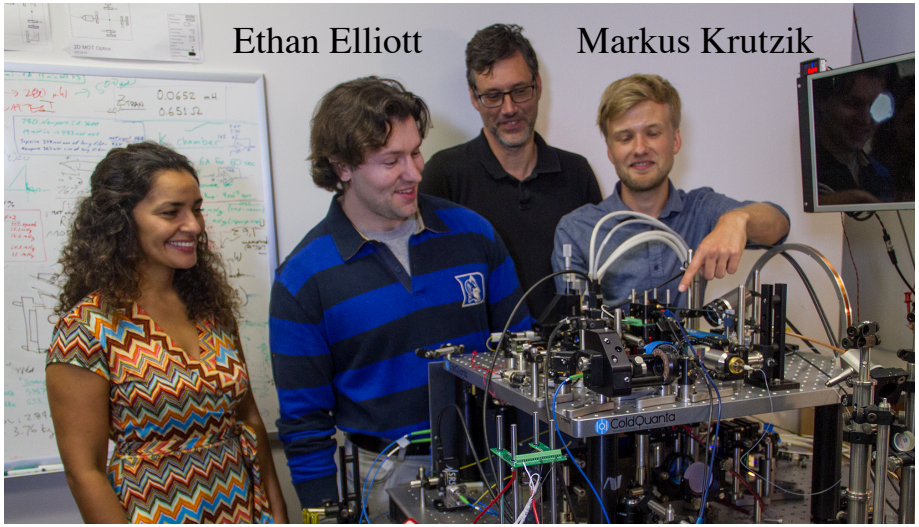

Special Thanks to:
Rob Thompson, Anita Sengupta, Kamal Oudrhiri, Sheng-wey Chiow, Nan Yu, and many more!

Thank You.

Backup Slides

Data Analysis

Differential cloud CM: $\Delta\bar{x} = \sum_i \left(\frac{n_{87,i}}{N_{87}} - \frac{n_{41,i}}{N_{41}}\right) x_i$

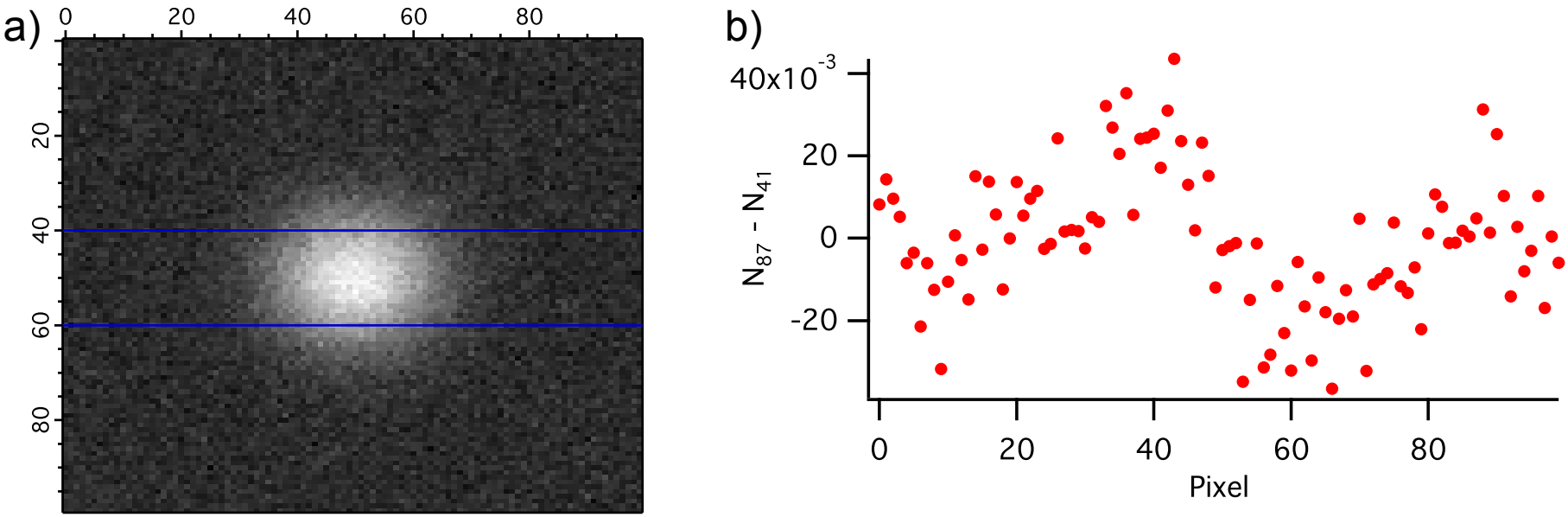

a) Simulated ^{87}Rb absorption image with **$N_{87} = 10^5$** and **0.035 OD noise/pixel**.

b) Line profile for differential ^{87}Rb and ^{41}K images with **40nm CM displacement**, vertically averaged over ROI (blue lines) and averaged over **10^3 measurements**.

Detect $\Delta x < 22$ nm ($\Delta v < 300$ nm/s)
for $N_{87} = N_{41} = 10^4$ and 1000 measurements.

Significance

Known sources that can limit the ultimate accuracy include: vibrations, rotations, accelerations, magnetic fields, differential center-of-mass position and velocity, ...

Assuming δv=1μm/s, δz=1μm, $\delta\Omega=10^{-3}\,\Omega_{ISS}$, a = 100 a_0, n_0 = 2 x 10^8/cm^3, 2T = 20s

Gravity gradient shifts

- Test masses traveling different classical paths (δr, δv) experience different gravitational potentials.

$$k_{eff}\gamma_{ZZ}(\delta z+\delta vT)T^2 = 3.0\times10^{-12}\,g$$

Detection Limits:

$\Delta v < 300$ nm/s ➔ nearly 3 × improvement

$\Delta x < 22$ nm ➔ nearly 100 × improvement

Error Budget Limits:

$\Delta v < 3$ nm/s ➔ nearly 10^3 × improvement

$\Delta x < 0.1$ nm ➔ nearly 10^4 × improvement

Significance

Known sources that can limit the ultimate accuracy include: vibrations, rotations, accelerations, magnetic fields, differential center-of-mass position and velocity, ...

Assuming δv=1μm/s, δz=1μm, $\delta\Omega=10^{-3}\,\Omega_{ISS}$, a = 100 a_0, n_0 = 2 x 10^8/cm^3, 2T = 20s

Gravity gradient shifts

- Test masses traveling different classical paths (δr, δv) experience different gravitational potentials.

$$k_{eff}\gamma_{ZZ}(\delta z+\delta vT)T^2 = 3.0\times10^{-12}\,g$$

Detection Limits:

$\Delta v < 300$ nm/s ➔ nearly 3 × improvement

$\Delta x < 22$ nm ➔ nearly 100 × improvement

Mitigation:

- Time-asymmetric Mach-Zehnder configuration (*i.e.* open AI)

$$k_{eff}\gamma_{zz}(z_i+\cancel{v_iT})T^2+\cancel{k_{eff}v_i\delta T}<10^{-14}\,g$$

$\delta T = \gamma_{zz}T^3$

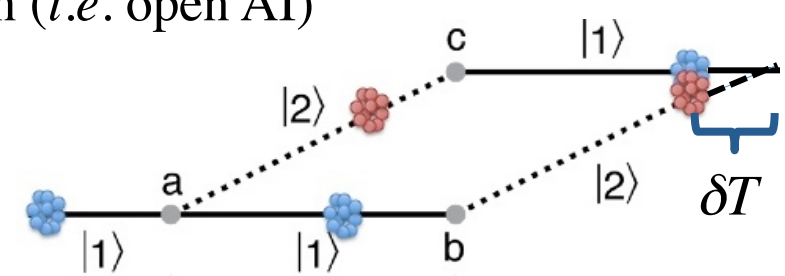

*A. Roura *et al.*, "Overcoming loss of contrast in atom interferometry due to gravity gradients" NJP, **16**, 123012 (2014)

Magnetic Field Error Budget

Preliminary Error Budget for ^{87}Rb and ^{41}K CM overlap

	Systematic	CM position	CM velocity	Comments
1	1st Order Zeeman	0.17nm	34nm/s	Mitigated by dissociating ^{41}K and ^{87}Rb to the clock states.
2	2nd Order Zeeman	< 0.1nm	2nm/s	Independent of B-field magnitude by field-direction modulation.

Assuming $B = 1$ Gauss and $\Delta B = 10$ mGauss/cm, detection 10ms after dissociation.

- Requires characterization of B and ΔB to a part in 10^3 using Stern-Gerlach and RF spectroscopy:

	1st Order Zeeman ($\|1,1\rangle$)	2nd Order Zeeman ($\|1,0\rangle$)
^{87}Rb	$1.6nm/ms^2$	$2.6pm/ms^2$
^{41}K	$3.4nm/ms^2$	$151pm/ms^2$

Magnetic field dependent accelerations for $B = 1$ Gauss and $\Delta B = 10$ mG/cm

- 2nd Order can be modulated to zero with B-field reversal due to:

$$F = 2\hbar\alpha B\Delta B$$

Magic Optical Trap Requirements

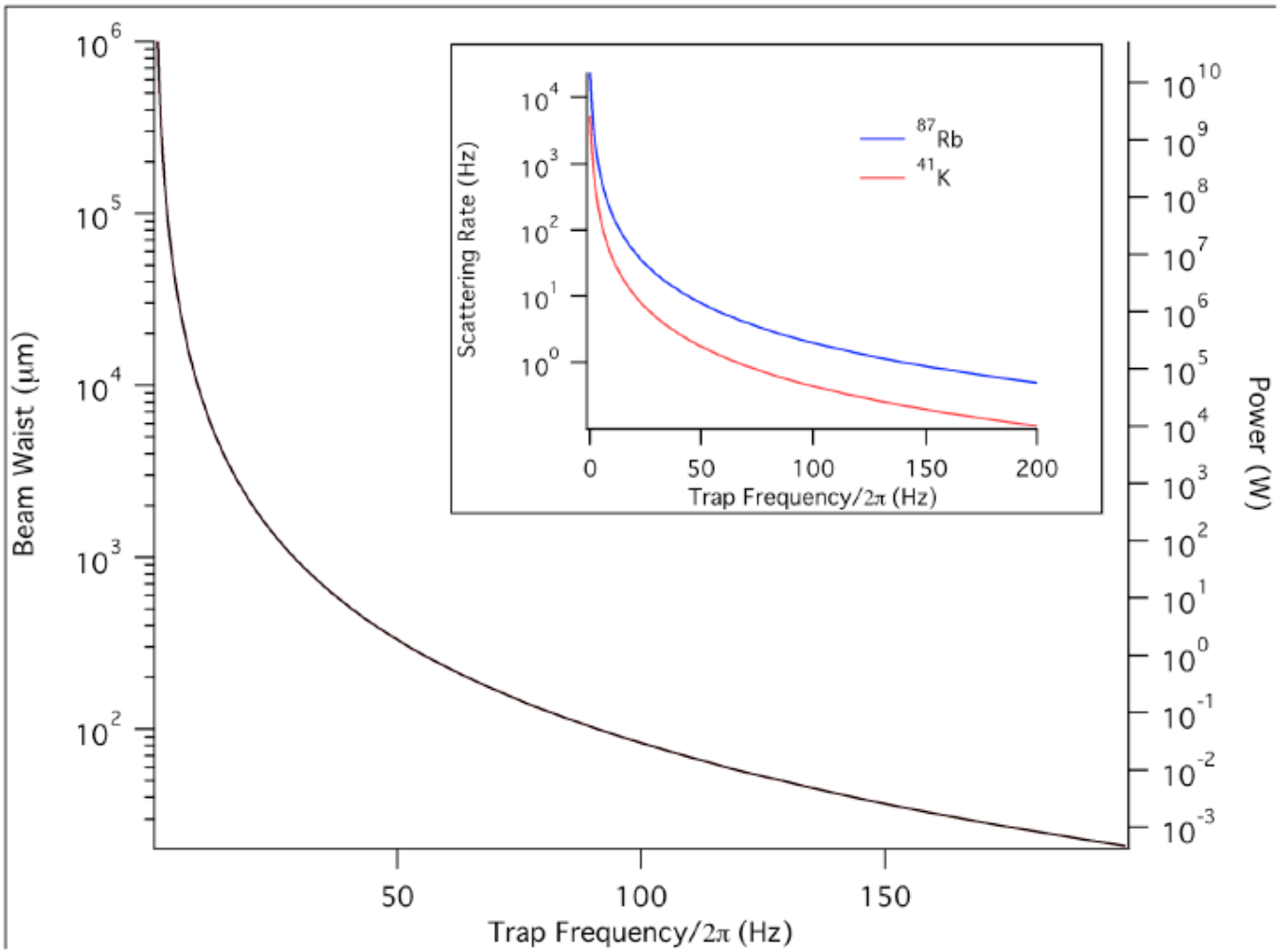

Figure 1: Calculated beam waist and optical power requirements as a function of the optical trap frequency for compensation of the earth's gravitational force, assuming a magic wavelength ODT for ^{87}Rb and ^{41}K with λ_{magic} ~ 812 nm. The insert gives the corresponding single-photon scattering rates for ^{87}Rb and ^{41}K.

Equations for contrast and number loss

In the point-source approximation, the contrast (over the entire cloud) is approximately given by the overlap integral of the temperature-dependent density profile of the atomic gas in free fall (n(x,y,t)) and the peak normalized excitation fraction (NEF(x,y,t)) of the final AI pulse.

where:

1) $$n(x,y,t) = \frac{1}{2\pi\left(\sigma_0^2 + \frac{k_B T}{m} t^2\right)} e^{-\frac{x^2+y^2}{2\left(\sigma_0^2 + \frac{k_B T}{m} t^2\right)}}$$

2) $$NEF(x,y,t) = A \sin^2\left(\Omega_0 e^{-2\frac{x^2+y^2}{w^2}} \frac{t}{2}\right)$$

Contrast and Loss functions of:

$$\boxed{\int n(x,y,t) * NEF(x,y,\pi/\Omega_0)\,dxdy}$$

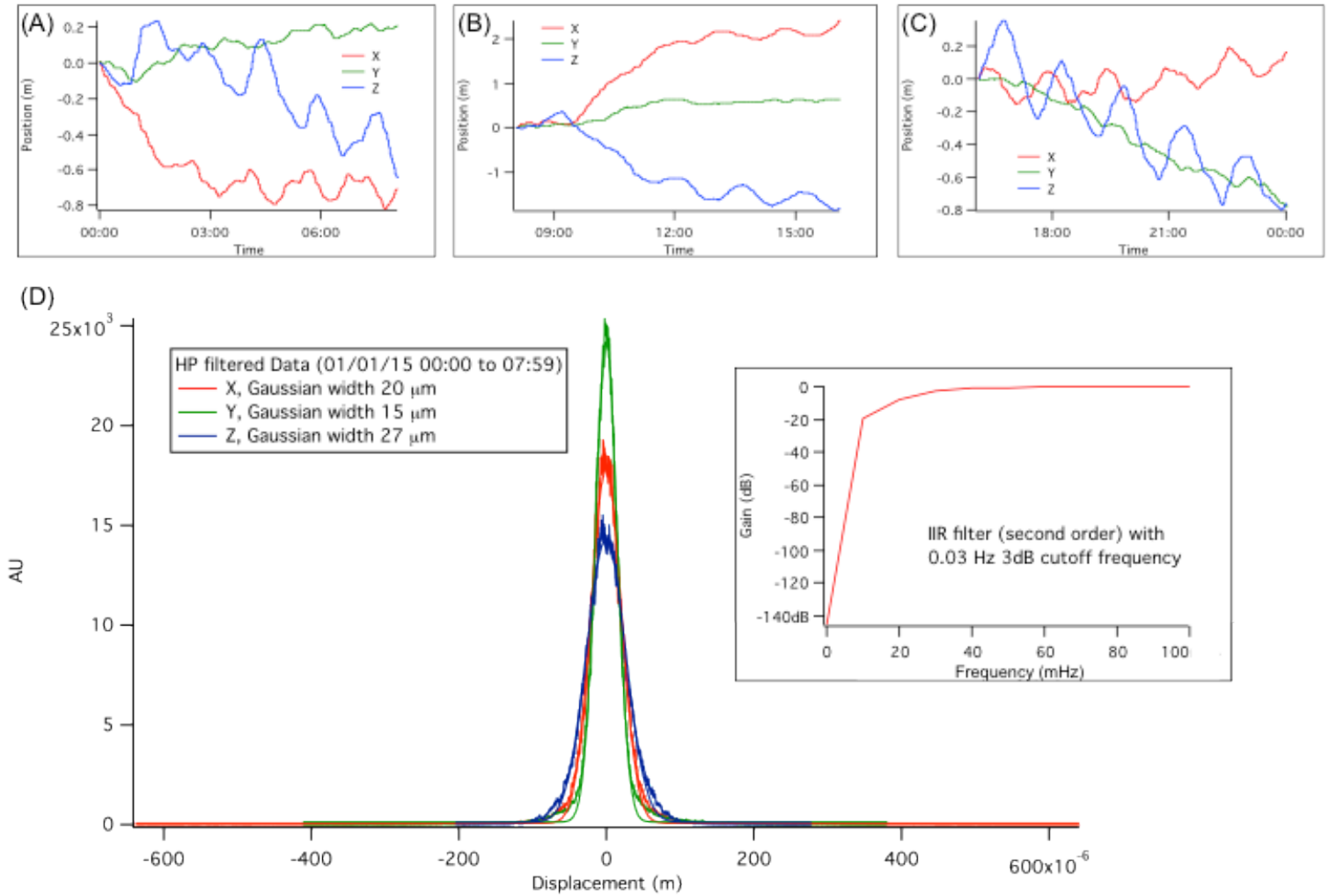
(A)
Position (m)
Time
X
Y
Z
(B)
Position (m)
Time
X
Y
Z
(C)
Position (m)
Time
X
Y
Z
(D)
HP filtered Data (01/01/15 00:00 to 07:59)
X, Gaussian width 20 μm
Y, Gaussian width 15 μm
Z, Gaussian width 27 μm
AU
Displacement (m)
IIR filter (second order) with
0.03 Hz 3dB cutoff frequency
Gain (dB)
Frequency (mHz)

(E)

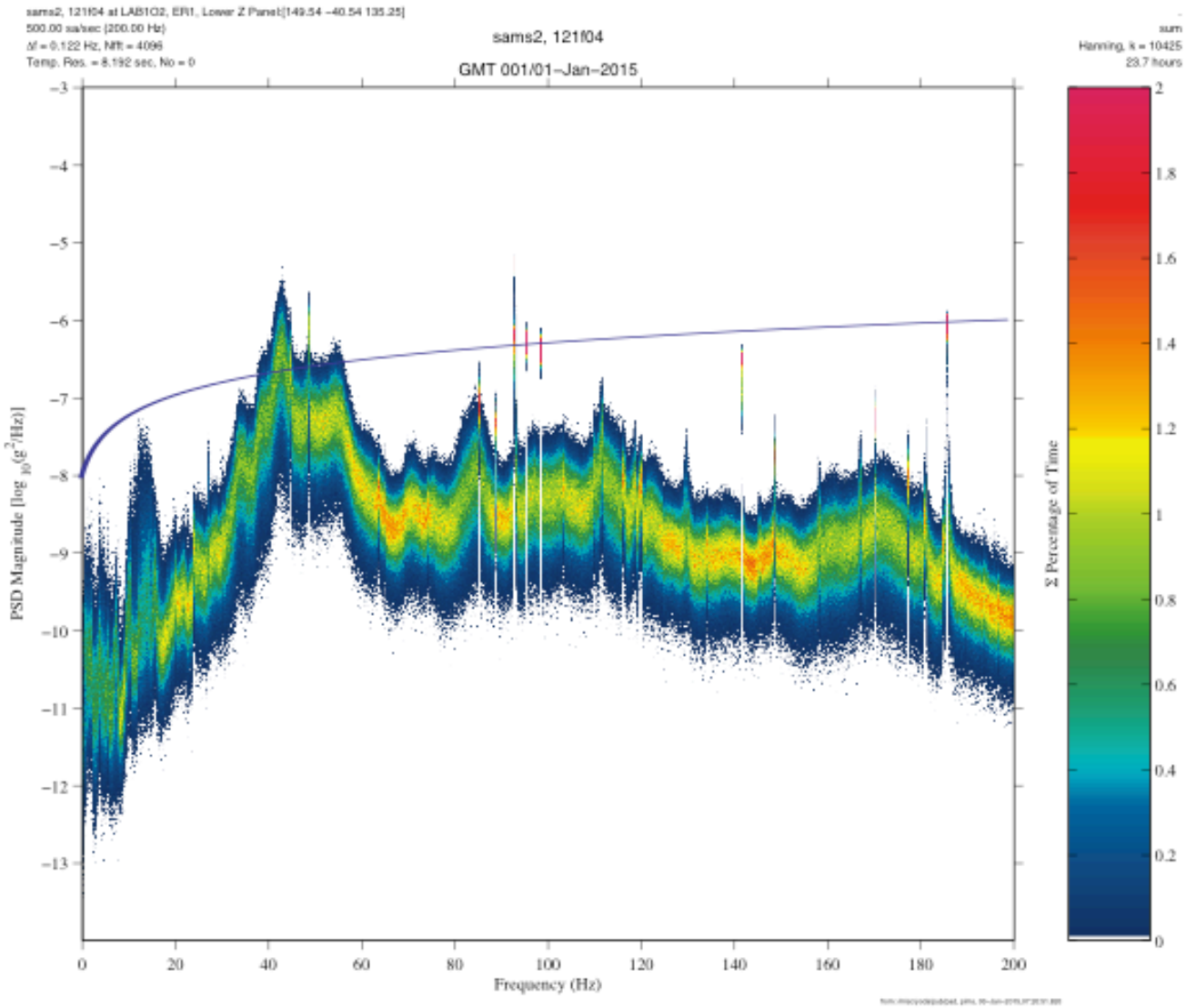
sams2, 121f04 at LAB1O2, ER1, Lower Z Panel:[149.54 -40.54 135.25]
500.00 sa/sec (200.00 Hz)
Δf = 0.122 Hz, Nfft = 4096
Temp. Res. = 8.192 sec, No = 0
sams2, 121f04
GMT 001/01-Jan-2015
sum
Hanning, k = 10425
23.7 hours
PSD Magnitude [log10(g²/Hz)]
Frequency (Hz)
% Percentage of Time

RF Rabi Frequency

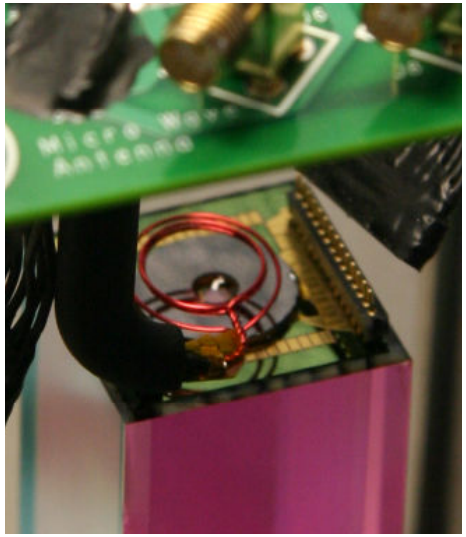

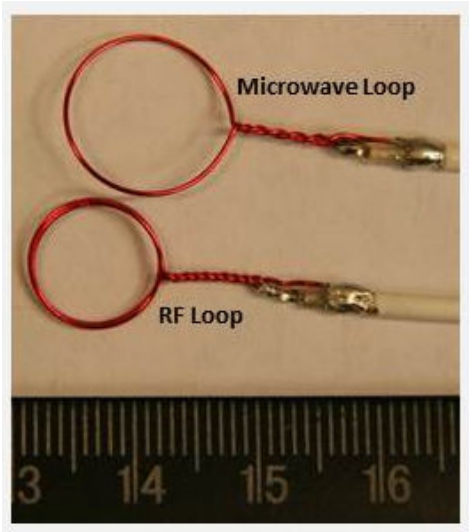

➢ Adiabatic rapid passage calibration suggest > 20 kHz well within grasp (sub-1W) (F=2 helps?)

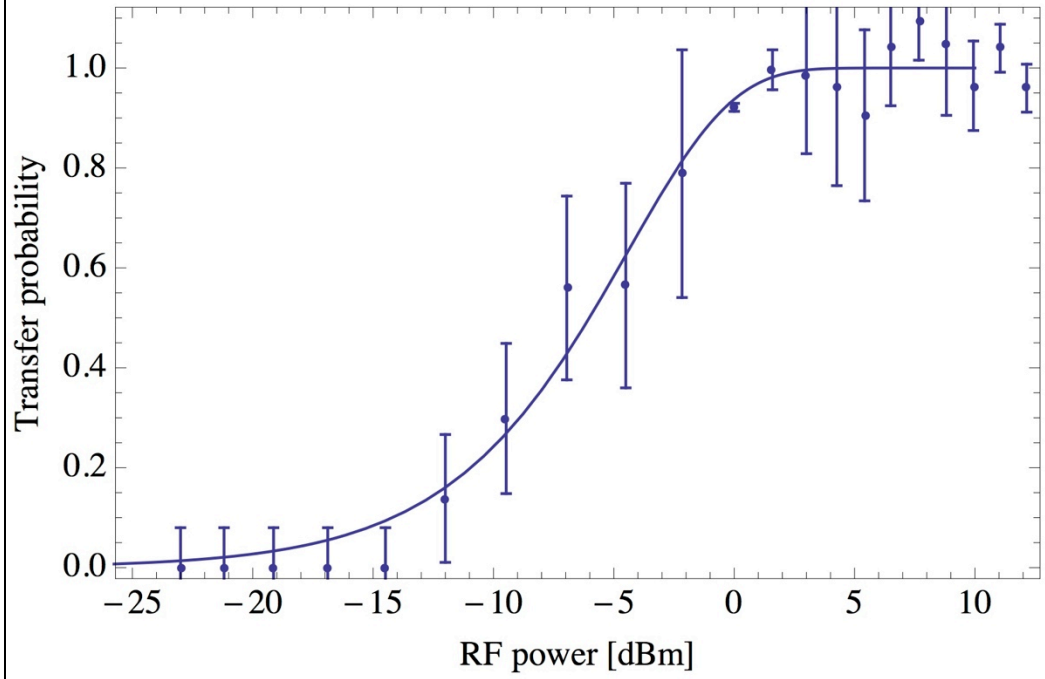

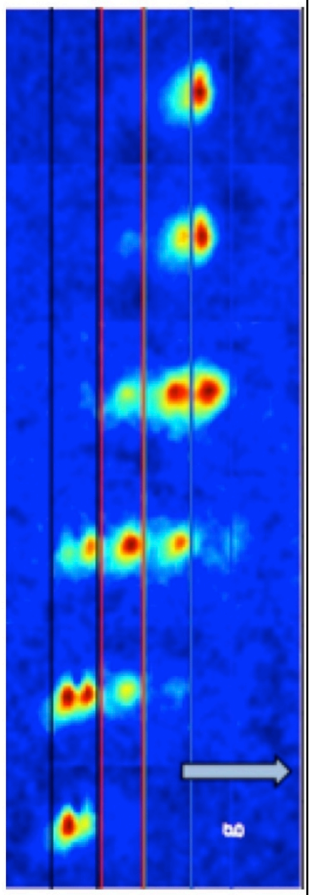

sweep~0.5 Mhz/ms

41

Data Analysis

- Correlations in dissociated FM

$$p_1 = -p_2 = \sqrt{m_i \hbar \delta}$$

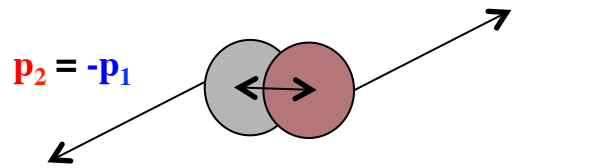

Dimer Size: $\langle r \rangle = a/2$

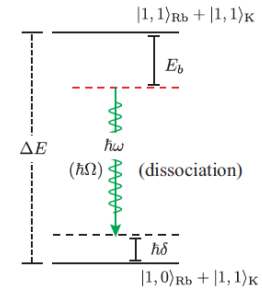

PRL 94, 110401 (2005) PHYSICAL REVIEW LETTERS week ending 25 MARCH 2005

Probing Pair-Correlated Fermionic Atoms through Correlations in Atom Shot Noise

M. Greiner,* C. A. Regal, J. T. Stewart, and D. S. Jin†

- Fine-structure extracted from noise correlations:

$$\mathcal{G}_{\alpha\beta}(\mathbf{r},\mathbf{r}') = \langle \hat{n}_\alpha(\mathbf{r})\hat{n}_\beta(\mathbf{r}')\rangle_t - \langle \hat{n}_\alpha(\mathbf{r})\rangle_t \langle \hat{n}_\beta(\mathbf{r}')\rangle_t.$$

  – Correlations in rotation-angle of images insitu & TOF

Momentum-Space

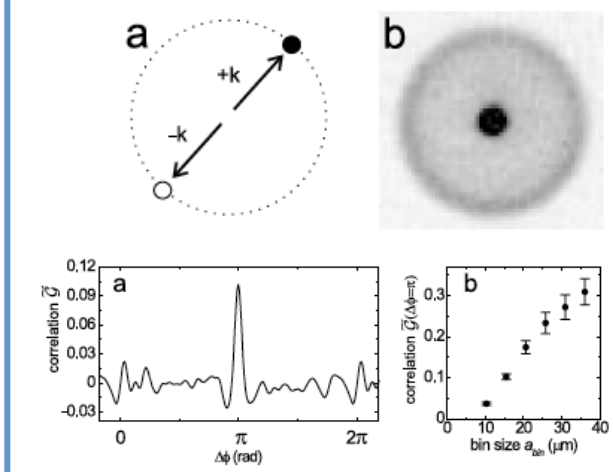

Position-Space

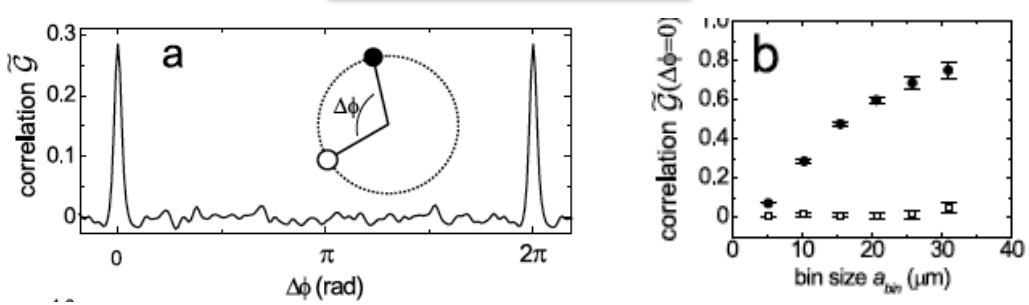

US/UK World Magnetic Model - Epoch 2015.0
Main Field Total Intensity (F)

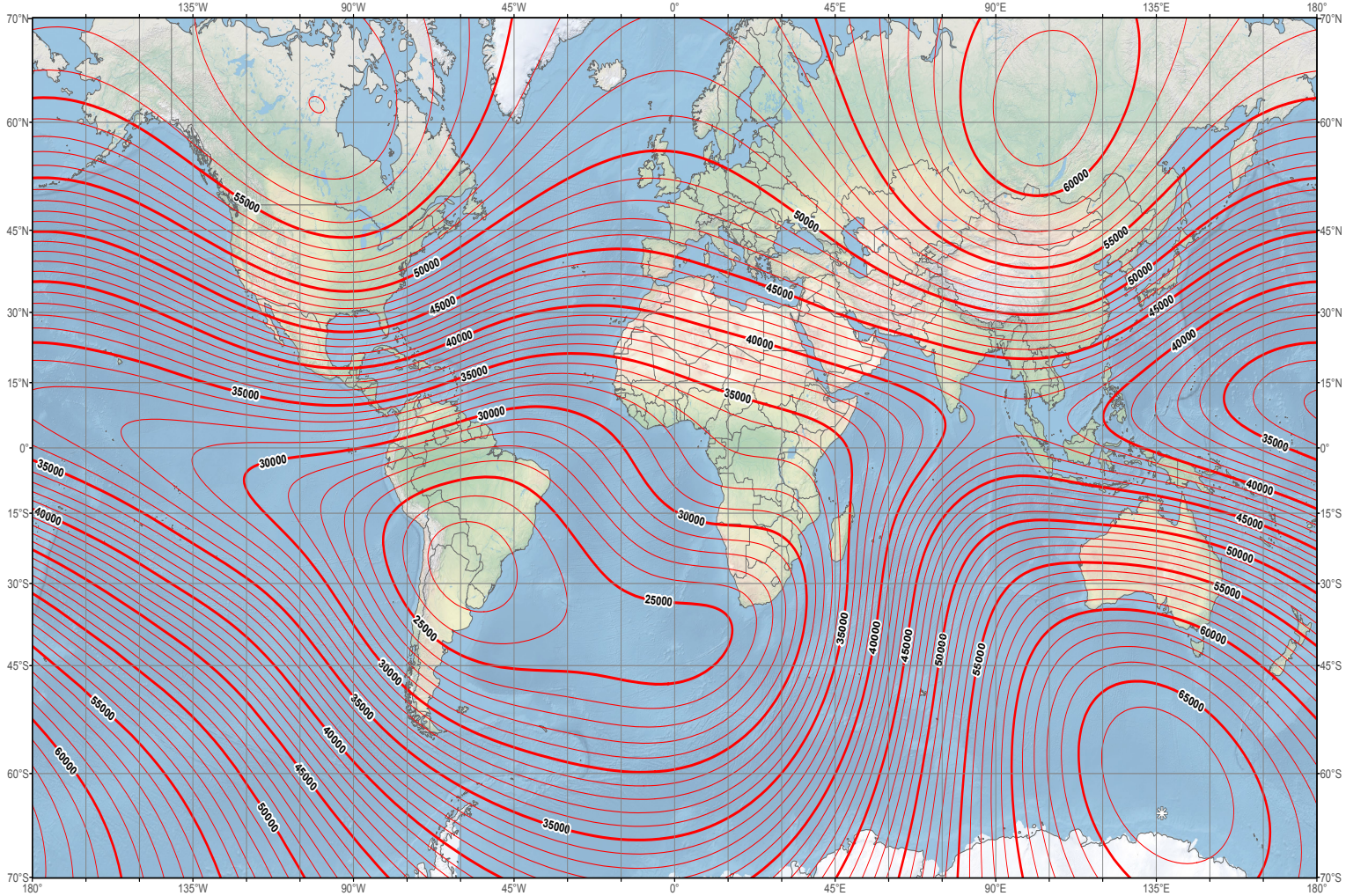

Main Field Total Intensity (F)
Contour interval: 1000 nT.
Mercator Projection.
: Position of dip poles

Map developed by NOAA/NGDC & CIRES
http://ngdc.noaa.gov/geomag/WMM
Map reviewed by NGA and BGS
Published December 2014

B (vertical/radial) intensity map

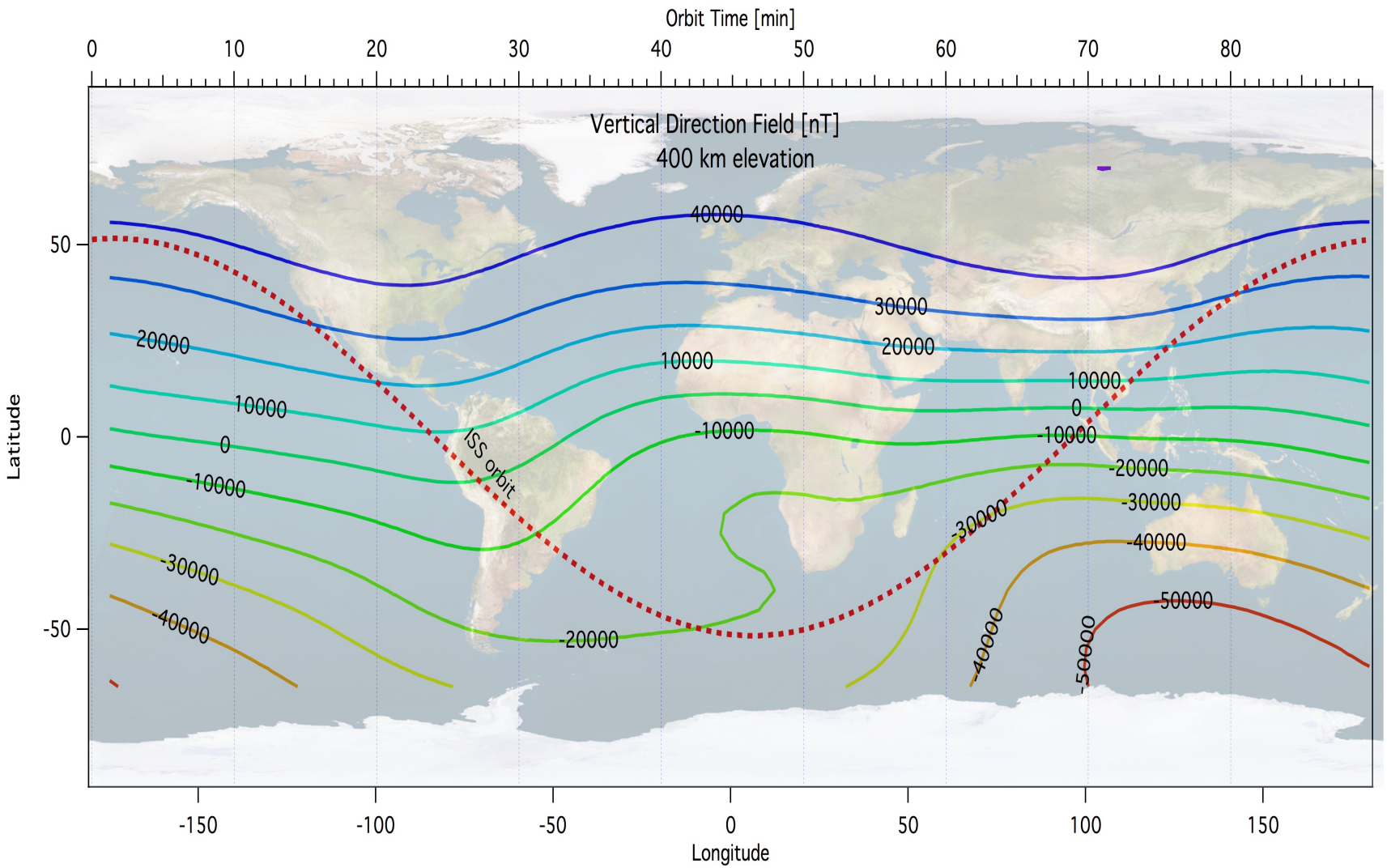

GTB Work

- Measure atom numbers and densities for ^{87}Rb and either ^{41}K or ^{39}K, sympathetically cooled to ~ T_C for both species.
  100 - 500 measurements over 1 – 3 days

- Characterize heteronuclear Feshbach molecule creation in a dual-species ^{87}Rb and ^{41}K gas using RF association.
  ~ 1000 measurements over 1 week

- Demonstrate and characterize purification schemes to remove free atoms from molecular gas.
  ~ 500 measurements over 3 days

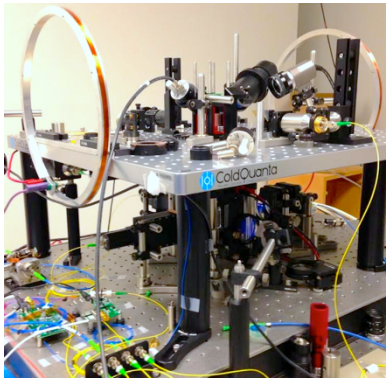

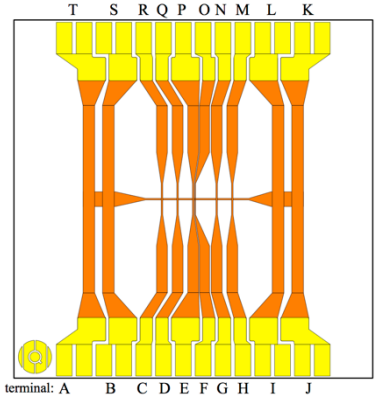

JPL's GTB lab model (left) with a flight-like vacuum system and a utility chip (right) offering an array of traces for a range of trap configurations, able to resemble the CAL atom chip traps.

- Characterize the ^{87}Rb and ^{41}K three body and atom-molecule loss spanning a range of fields from near resonance (B_0 = 38.4 Gauss) to near zero.
  ~ 1000 measurements over 1 week

- Measure the $|1,1\rangle \rightarrow |2,0\rangle$ microwave Rabi frequency for ^{41}K and explore the feasibility of making microwave + RF two-photon transitions to dissociate atoms into the $m_F = 0$ magnetically insensitive states
  $^{41}K|1,1\rangle +^{87} Rb|1,1\rangle \rightarrow^{41} K|2,0\rangle +^{87} Rb|1,0\rangle$.
  ~ 300 measurements over 2 days, up to 2000 measurements over 1 week for publishable data

- Demonstrate Bragg AI with single-species ^{87}Rb, dual-species ^{87}Rb-^{39}K, and ^{87}Rb-^{41}K.
  ~ 1000 - 2000 measurements over 1 week for characterization and optimization

- Image and characterize AI phase fringes artificially induced with short-T AIs.
  ~ 500 measurements over 3 days

Adiabatic Cooling

Atom Chip Metal – not to scale

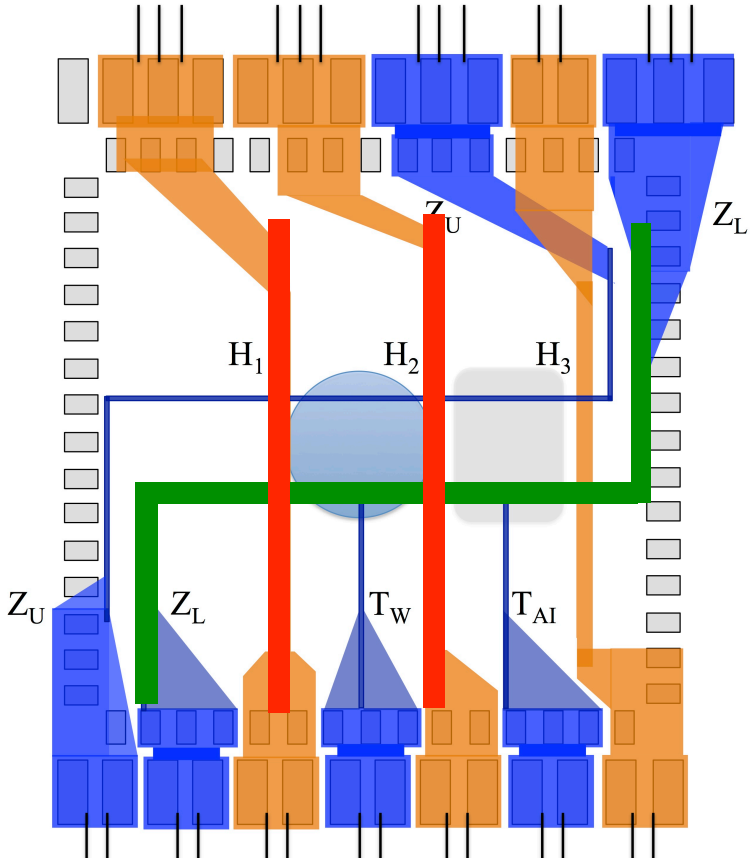

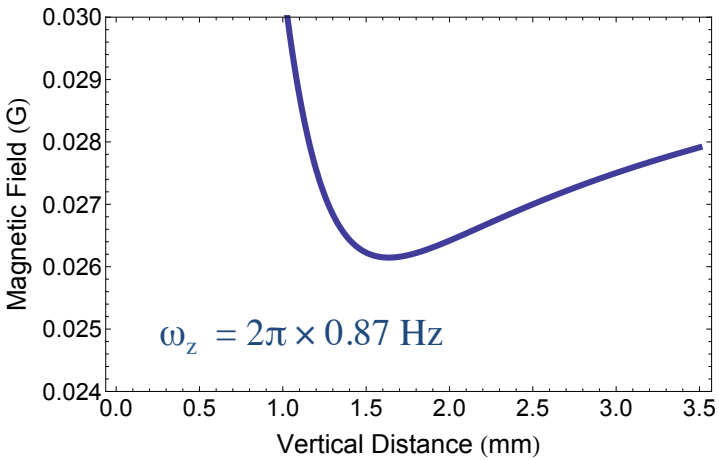

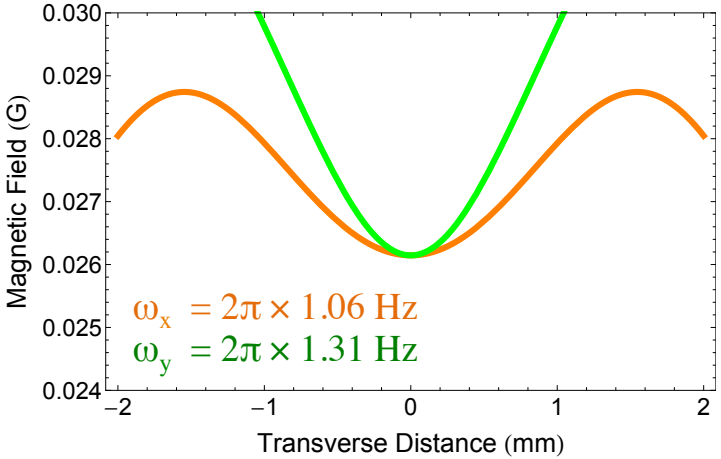

Low frequency, high symmetry trap:

$\overline{\omega_{Rb}} = 1.06$ Hz with trap ratio < 3:2

Z-wire = 23 mA
H-wires = 10mA
$B_x = 13$mG, $B_y = 27$mG

Light-pulse MZ Atom Interferometers

- Measurement based on an ensemble of effective 2-level systems, coupled with light pulses with opposite **k**-vectors (Doppler sensitive spectroscopy).
  - Raman pulses couple two electronic and momentum levels, $g_1 \neq g_2$, $k_{eff} = 2k$
  - Bragg pulses couple two momentum levels, same electronic, $g_1 = g_2$, $k_{eff} = 2nk$

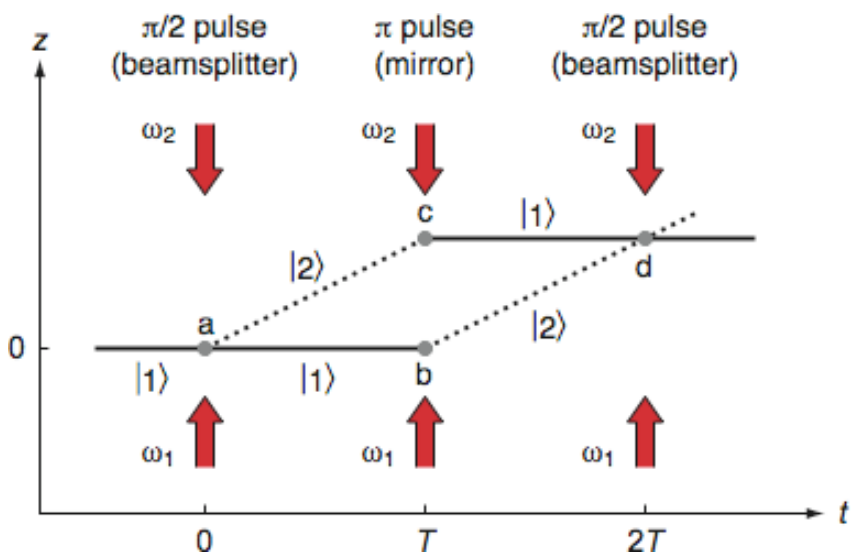

Fig. 1. Light-pulse atom interferometer diagram

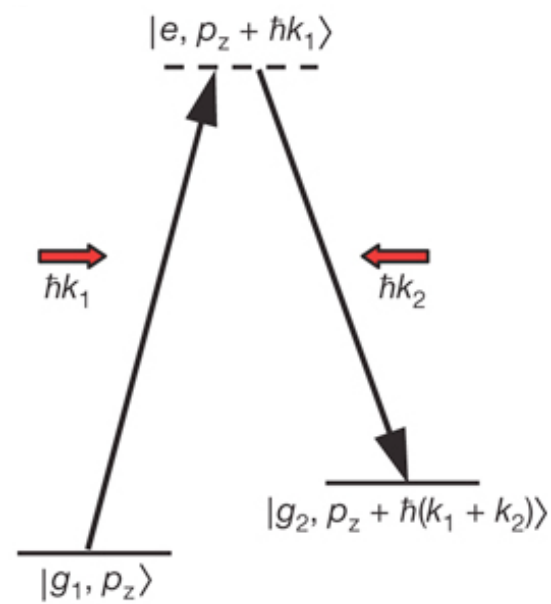

Two discrete energy and/or momentum states coupled with 2-photon transitions

Light-pulse MZ Atom Interferometers

- Measurement based on an ensemble of effective 2-level systems, coupled with light pulses with opposite **k**-vectors (Doppler sensitive spectroscopy).
  - Raman pulses couple two electronic and momentum levels, $g_1 \neq g_2$, $k_{eff} = 2k$
  - Bragg pulses couple two momentum levels, same electronic, $g_1 = g_2$, $k_{eff} = 2nk$

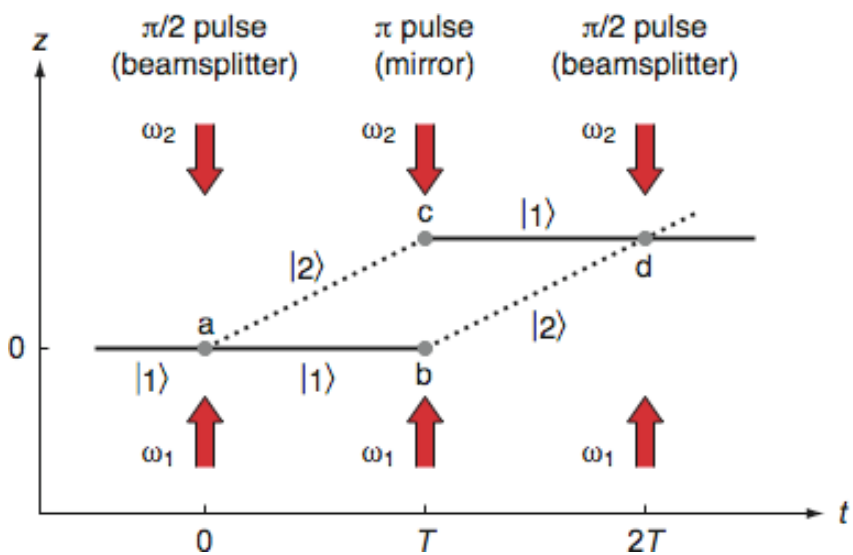

Fig. 1. Light-pulse atom interferometer diagram

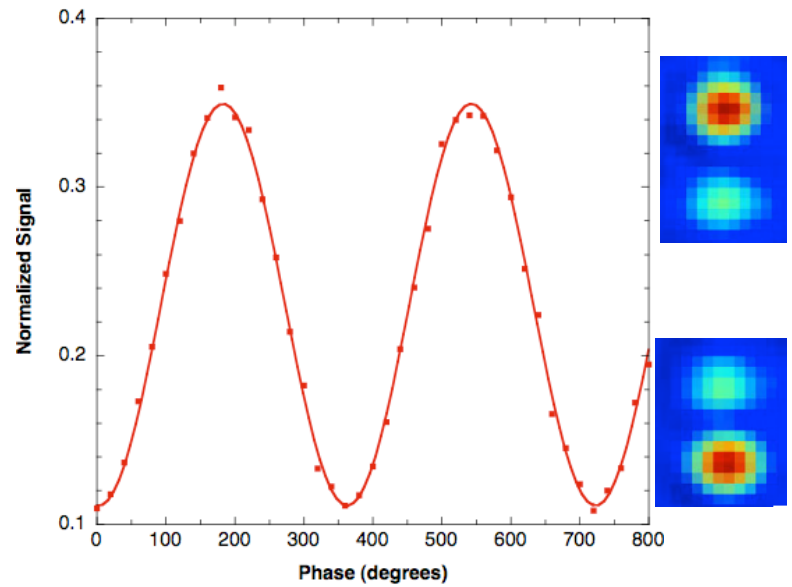

Fig. 2. Atom interferometer fringes as observed in our laboratory prototype instrument [6]. The phase of the final Raman π/2 pulse was scanned to generate the characteristic interferometer fringe.

Sensitive to inertial forces and rotations

$$\Delta\Phi_a = k_{\text{eff}} \cdot aT^2$$

$$\Delta\Phi_{rot} = 2m(\Omega \cdot A)/\hbar$$

Simple phase readout from final atomic states:

$$P = \frac{1}{2}(1 - \cos(\Delta\Phi))$$

Differential AI Measurements

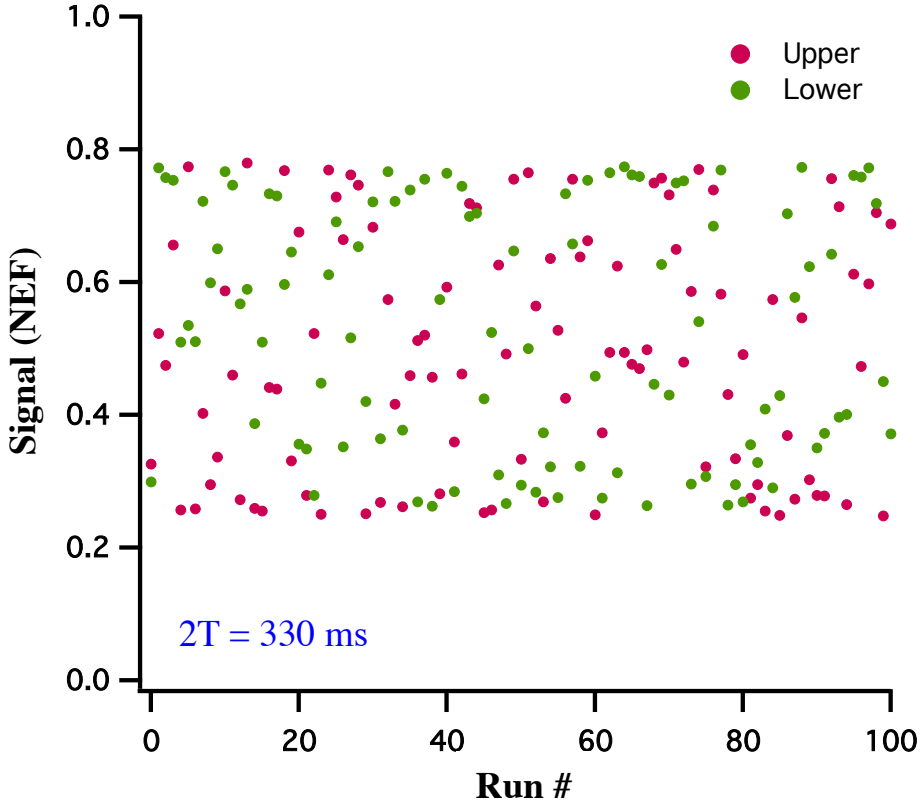

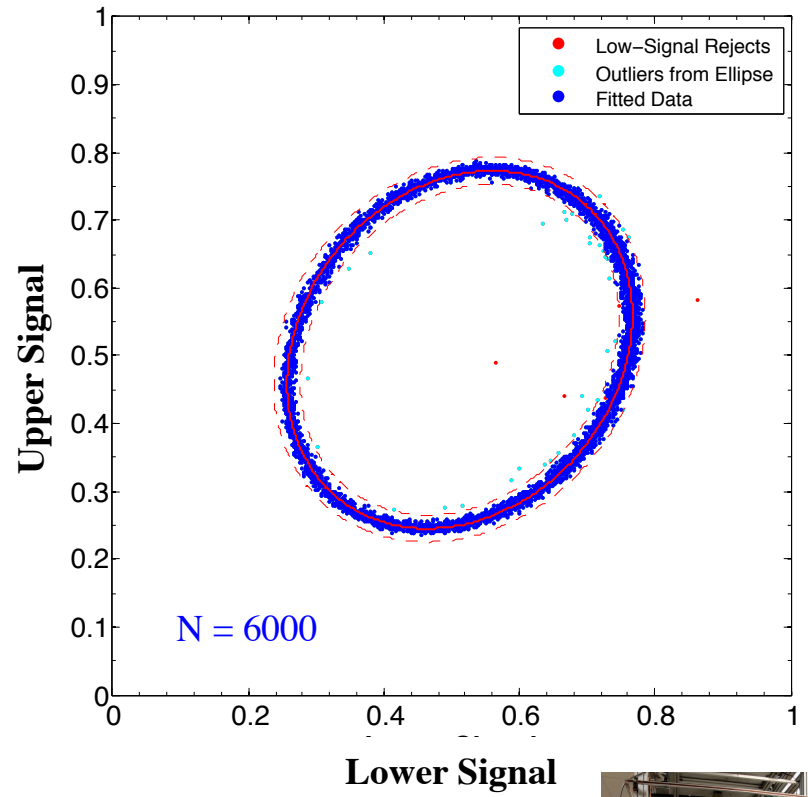

Left: Interferometer fringes for the two chambers of the gravity gradiometer.

Right: Parametric plot of correlations in the atom interferometer signals.

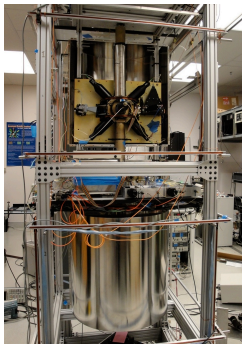

Feshbach Association

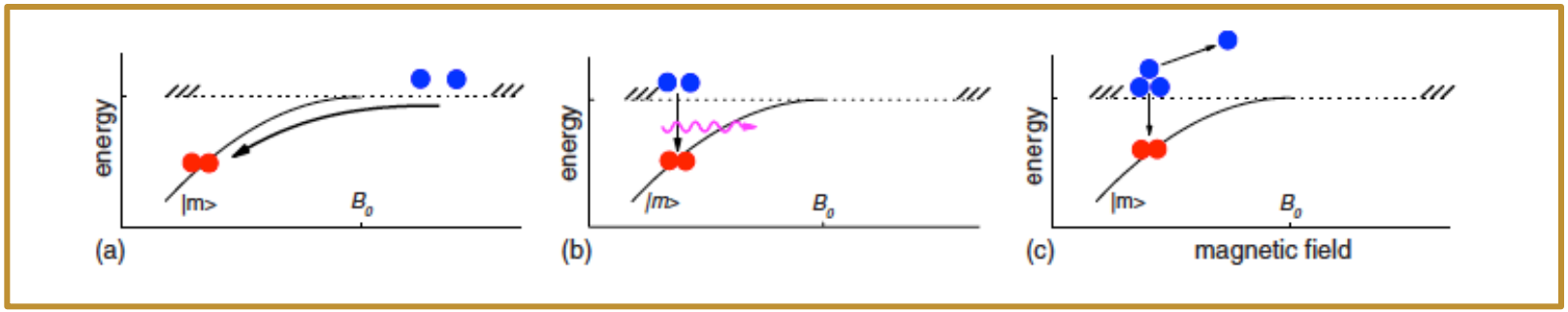

- Three primary methods for associating FRs:
  - Adiabatic field ramp
  - RF association
  - Three-body collisions

- Purification:
  - Stern-Gerlach
  - Resonant light "blow-away"

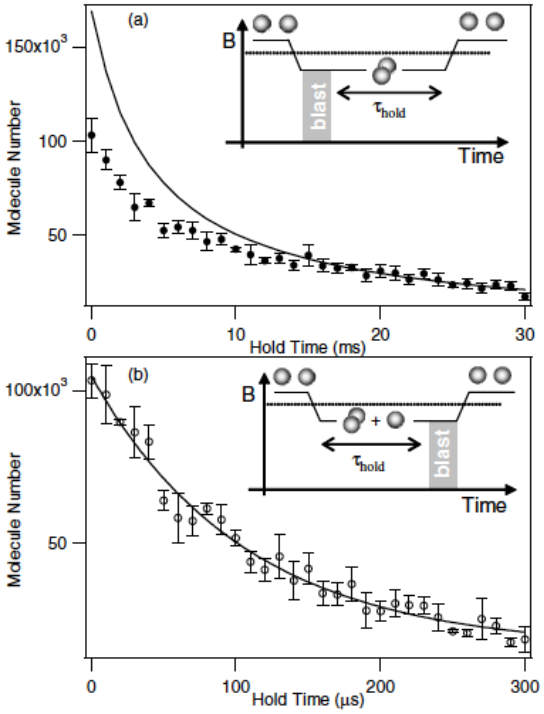

FIG. 37. Fast collisional decay of $^{23}Na_2$ Feshbach molecules. The molecules are trapped (a) alone or (b) together with atoms. From Mukaiyama *et al.*, 2004.

RF Feshbach Association

PHYSICAL REVIEW A 78, 061601(R) (2008)

Association of ultracold double-species bosonic molecules

C. Weber,[1,3] G. Barontini,[1] J. Catani,[1,2] G. Thalhammer,[1] M. Inguscio,[1,2] and F. Minardi[1,2]

$^{41}K - ^{87}Rb$

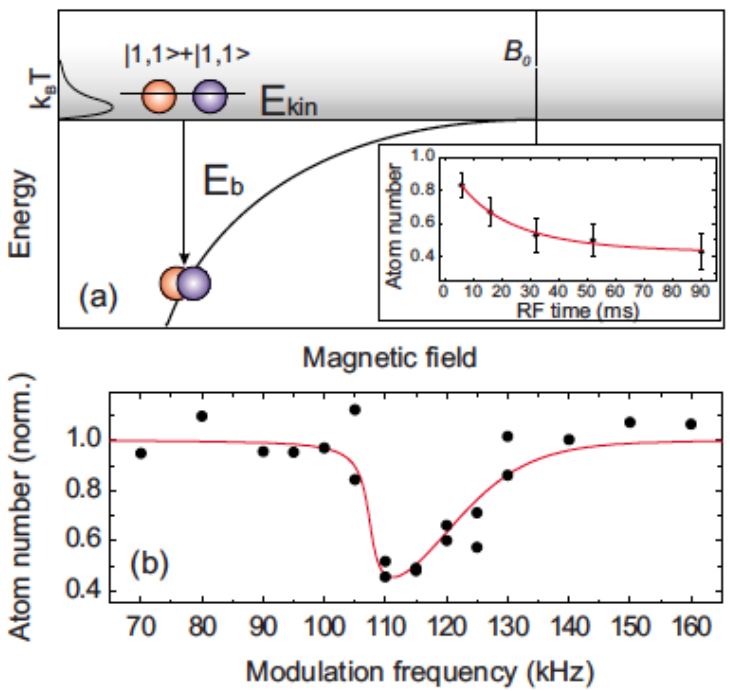

FIG. 1. (Color online) (a) Molecular radio-frequency association: two free atoms with relative kinetic energy E_{kin} are resonantly transferred to a molecular level by modulating the magnetic field. The inset shows the remaining atom number after a variable association time. The solid line is an nonexponential fit to data (see text). (b) Spectrum for an association time of 30 ms, B=78.25 G. The solid line is a fit with the line shape described in the text.

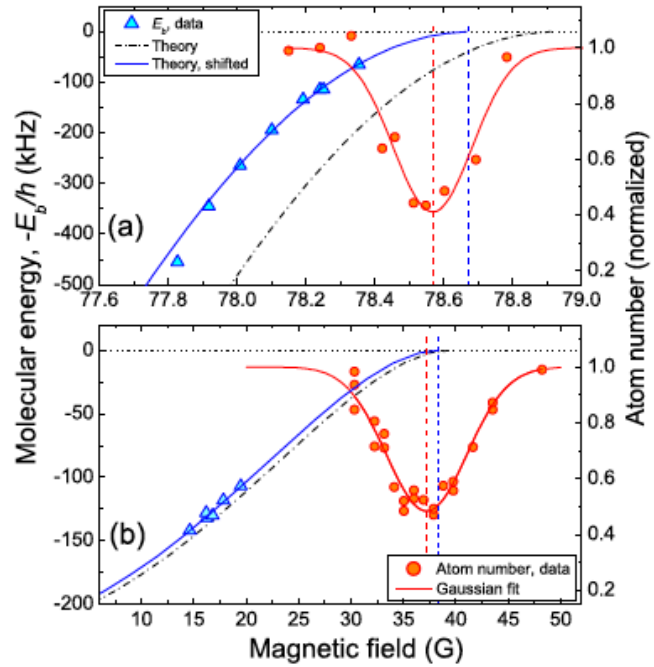

FIG. 2. (Color online) (a) KRb binding energy and three-body losses for the Feshbach resonance at 79 G: triangles show the experimental binding energies, circles the atom number. The dash-dotted black line shows the theoretical prediction for E_b; the solid blue line is the same curve, but translated by −0.24G. The solid red line represents a Gaussian fit to the atom number. The vertical dashed lines show the position of the FR as determined by the three-body losses (red, left) and the binding energy (blue, right). (b) Same as above, for the FR at 39 G. Note the widely different scale of x axis. Here the theoretical model for E_b is shifted by −1G.

Microgravity Justification # 1

Adiabatic conversion efficiency

PRL 97, 180404 (2006) PHYSICAL REVIEW LETTERS 3 NOVEMBER 2006

Observation of Heteronuclear Feshbach Molecules from a ^{85}Rb–^{87}Rb Gas

S. B. Papp* and C. E. Wieman
JILA, National Institute of Standards and Technology and University of Colorado, Boulder, Colorado 80309-0440, USA
(Received 3 August 2006; published 31 October 2006)

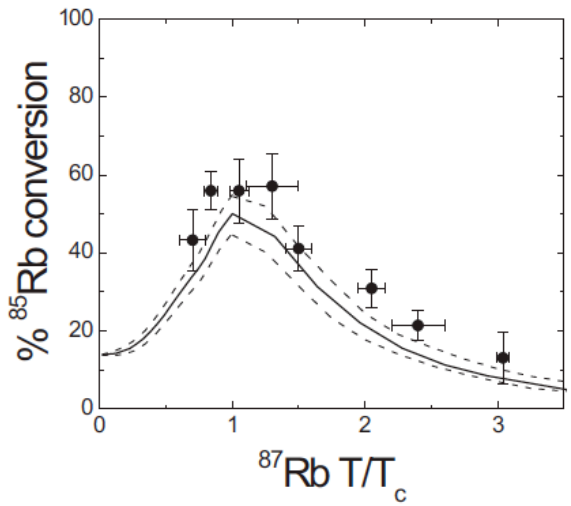

Figure 6.6: Heteronuclear molecule conversion efficiency at the 265 G Feshbach resonance as a function of ^{87}Rb T/T_c. At our largest conversion efficiency the ^{85}Rb gas has $T/T_c = 2.6$. The solid line shows a simulation based on our conversion model, and the dashed lines represent the uncertainty. The conversion drops below $T/T_c = 1$ since the BEC is spatially smaller than the thermal ^{85}Rb gas and the conversion process depends on the proximity of two atoms in phase space. Some of the data for this figure has been

Conversion efficiency scales with PSD α $n_0/T^{3/2}$

Molecular lifetimes

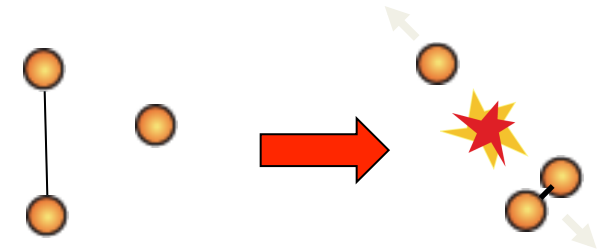

Atom-dimer collisions limit FR molecule lifetimes.

$$\frac{d}{dt}n_A = \frac{d}{dt}n_D = -\beta n_A n_D$$

Additional loss mechanisms from dimer-dimer collisions

Loss scales with n_0^2

FR dimers optimized for low T and low n_0

Purification

- *Stern-Gerlach purification*:
  - Unbound rubidium and potassium atoms in a magnetic field gradient (ΔB) are accelerated as:

	1st Order Zeeman ($\|1,1\rangle$)	2nd Order Zeeman ($\|1,0\rangle$)
^{87}Rb	$160nm/ms^2 \times \Delta B$	$260pm/ms^2 \times B\Delta B$
^{41}K	$340nm/ms^2 \times \Delta B$	$15.1nm/ms^2 \times B\Delta B$

where B is in Gauss and ΔB is in mGauss/cm.

  - The acceleration of the FM is:

$$\mathbf{a_{mol} = \mu_{mol}\Delta B/M_{mol}}$$

where: $M_{mol} = M_{Rb} + M_K$ and $\mu_{mol} \cong \mu_{Rb} + \mu_K$

Assuming $\Delta B \sim 20$ Gauss/cm and t = 30ms: Millimeter separations of ^{87}Rb, ^{41}K, and ^{87}Rb-^{41}K (>> few 0.1 mm cloud widths).

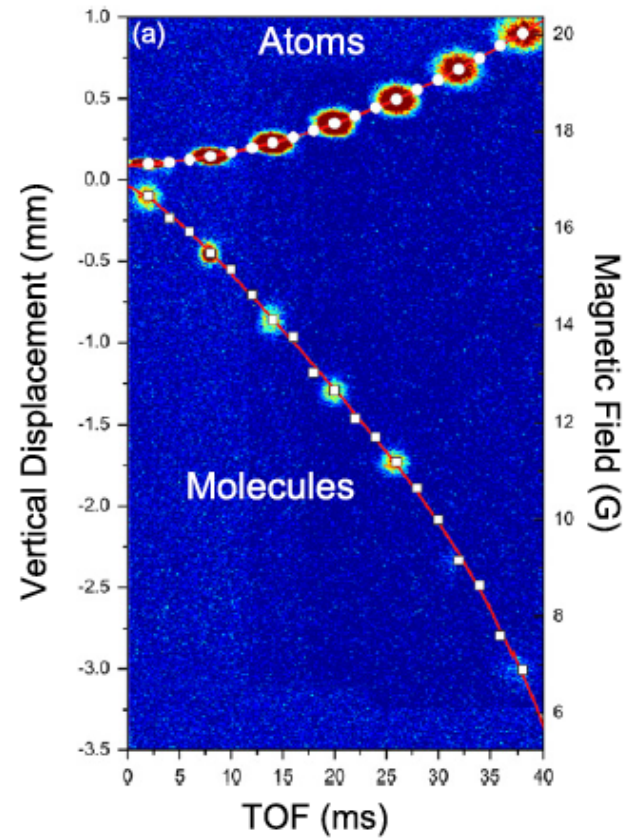

Stern-Gerlach separation of Cs_2 molecules from a BEC. Figure from M. Köppinger *et al*. (2014) NJP **16**, 115016

Purification

Resonant light purification:

- Selective transition of ^{87}Rb and ^{41}K atoms from F = 1 ➔ F = 2 with low-intensity microwave.
- High-intensity "blast" light resonant with F = 2 ➔ F = 3 transition.
- High selectivity of this double-resonance method minimizes molecular heating/loss.*

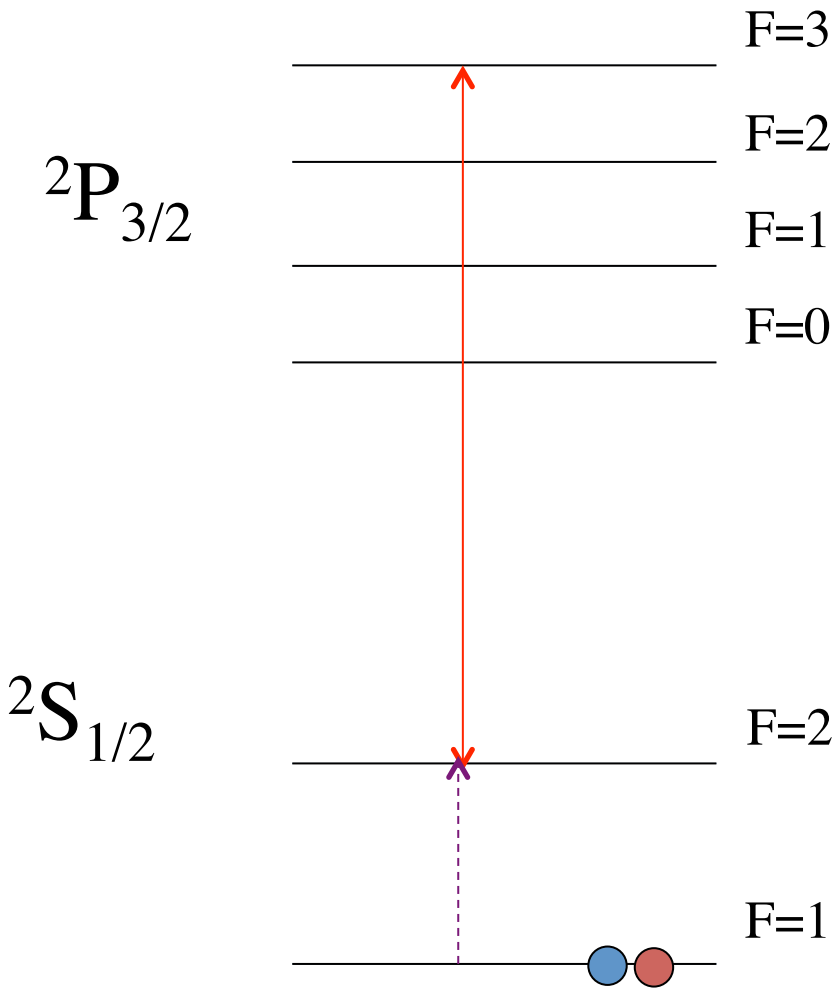

*F. Lang *et al*., "Long-lived feshbach molecules in a three-dimensional optical lattice" PRL, **96**, 050402 (2006)

Dual-Species AI

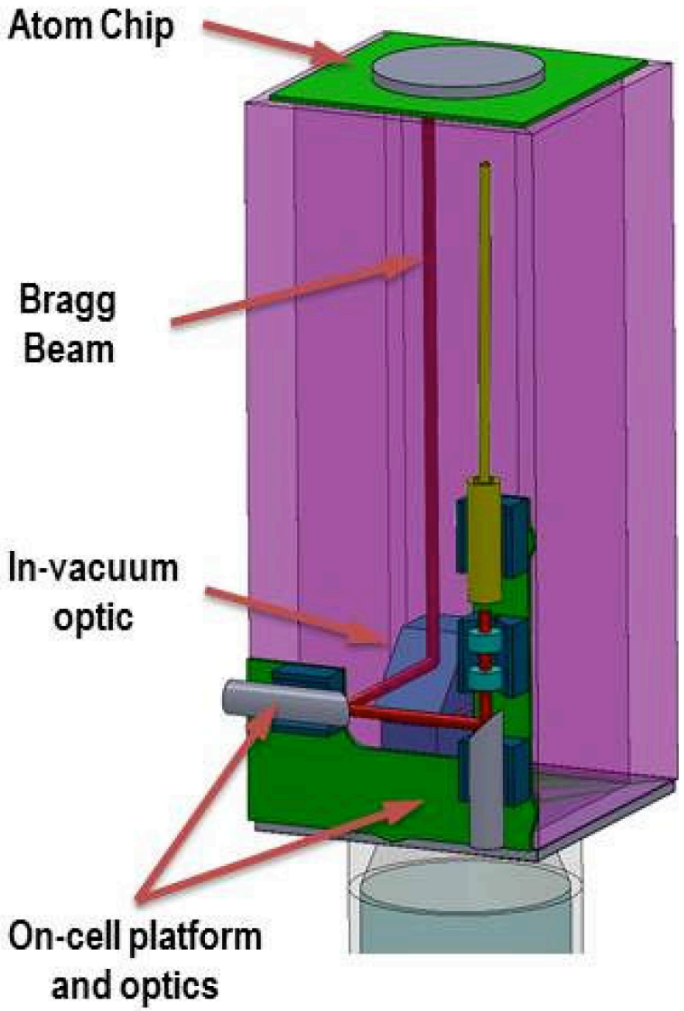

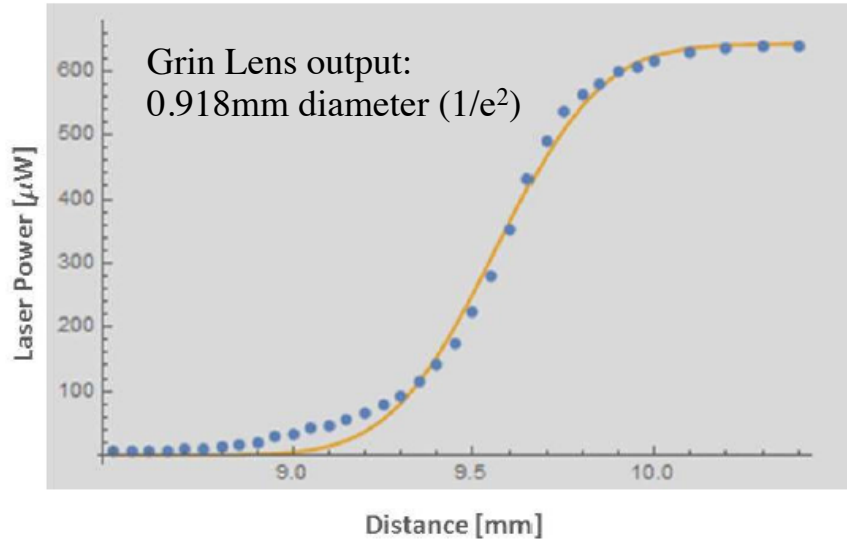

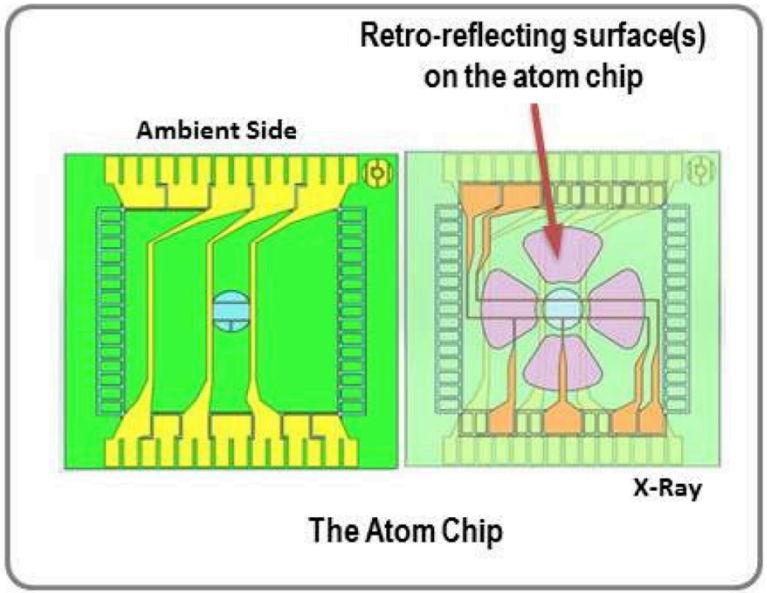

Contrast Study

Contrast and atom loss from thermal expansion in 1mm ($1/e^2$) Bragg beam:

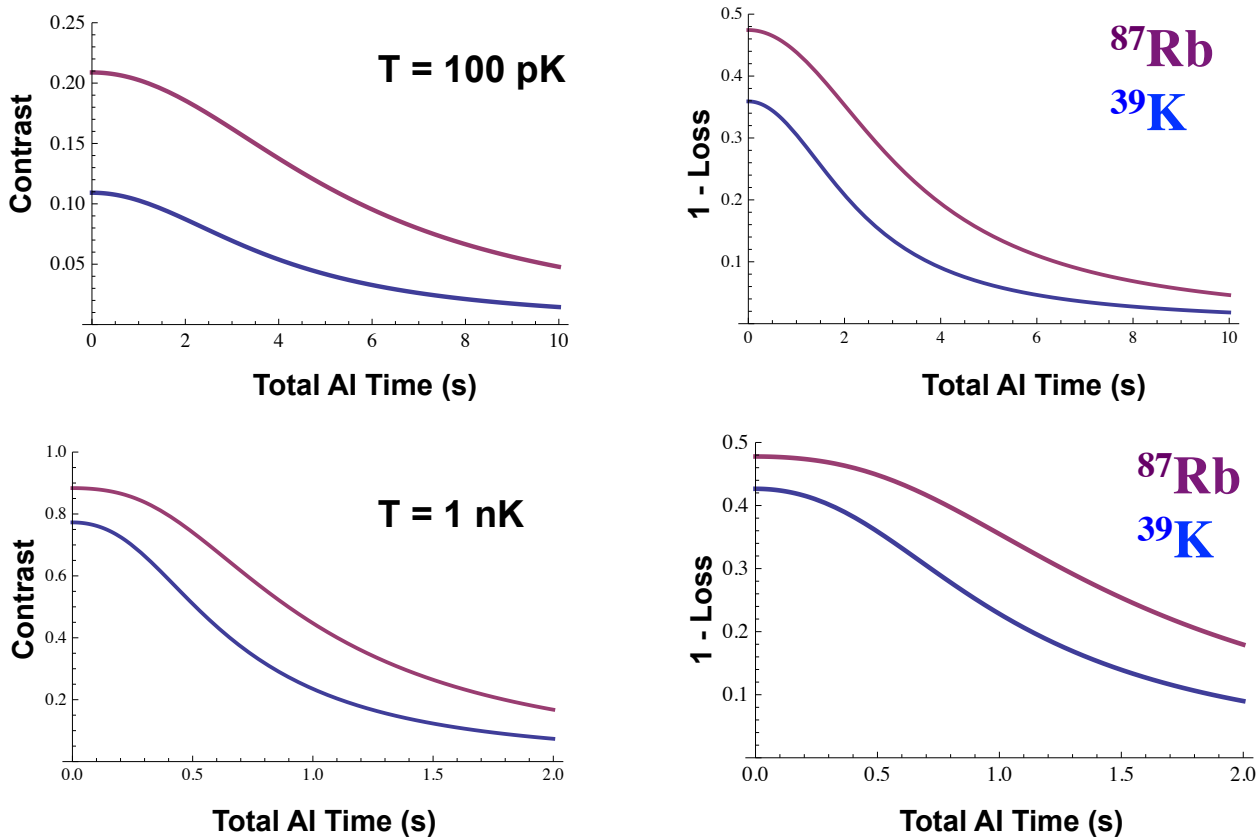

Contrast loss from thermal Doppler width of atoms:

	^{87}Rb at 1nK	^{87}Rb at 100pK	^{39}K at 1nK	^{39}RK at 100pK
Doppler Width	394 Hz	125 Hz	589 Hz	186 Hz
Peak NEF^3	0.798	0.977	0.622	0.949

Vibration Requirements

Vibrations are considered for:

1) Possible atom loss from colliding with vacuum chamber wall.

Negligible ISS relative motion over 20s from SAMS acceleration data for the 121F04 three-axis sensor on 01/01/2015.

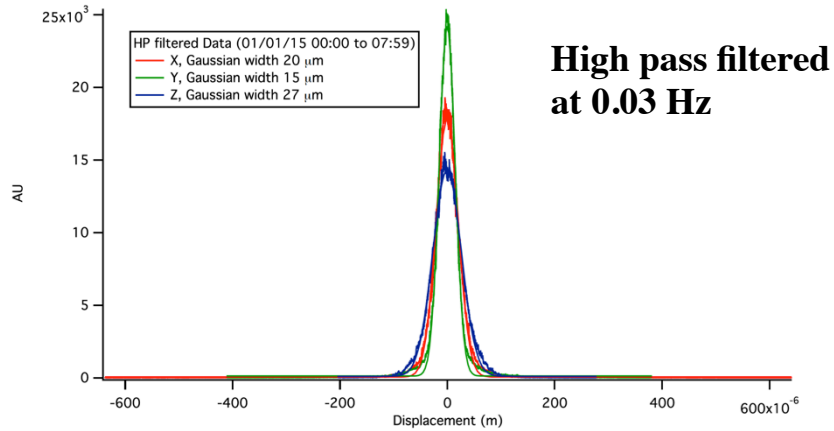

2) Doppler shift when light reflects off a vibrating mirror, need to be constrained less than Bragg diffraction bandwidth.

- A 100μs Gaussian Bragg pulse has a bandwidth of 10kHz.
- Less than 0.4kHz RMS Doppler shift (30% Bragg Rabi Frequency) requires < 10^{-8} g^2/Hz acceleration noise at 1Hz.

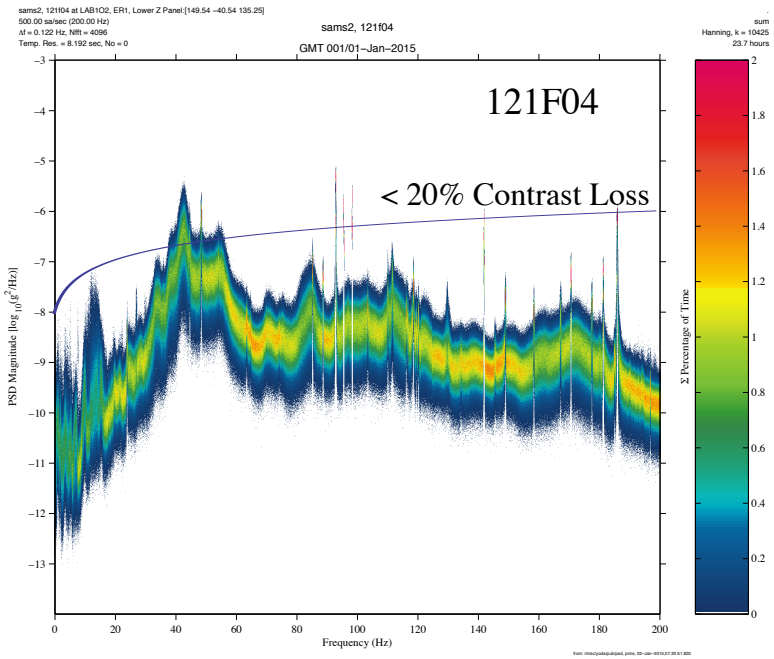

Feshbach Molecule CM Filtering

#1:

Low-energy Feshbach physics to prepare highly-overlapped dual-species atomic gases in microgravity

- Negate all systematics scaling with δr and δv.
- Molecular state-control at k_B*1 nK.

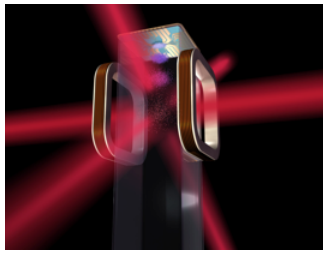

Key:
Fully symmetric quantum (s-wave) molecules assure no biases in dimer CM.

After disassociation, *for each particle-pair*, the positions (δr) are correlated and momenta (δp) anti-correlated*.

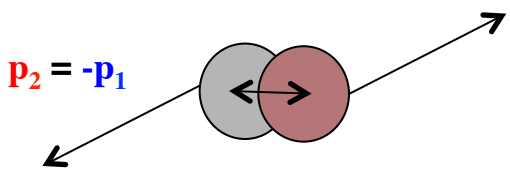

Dimer Size: $\langle r \rangle = a/2$

At $a = 3500a_0$ and T = 1nK,
δv ~ 750 μm/s and $\langle r \rangle = 200nm$

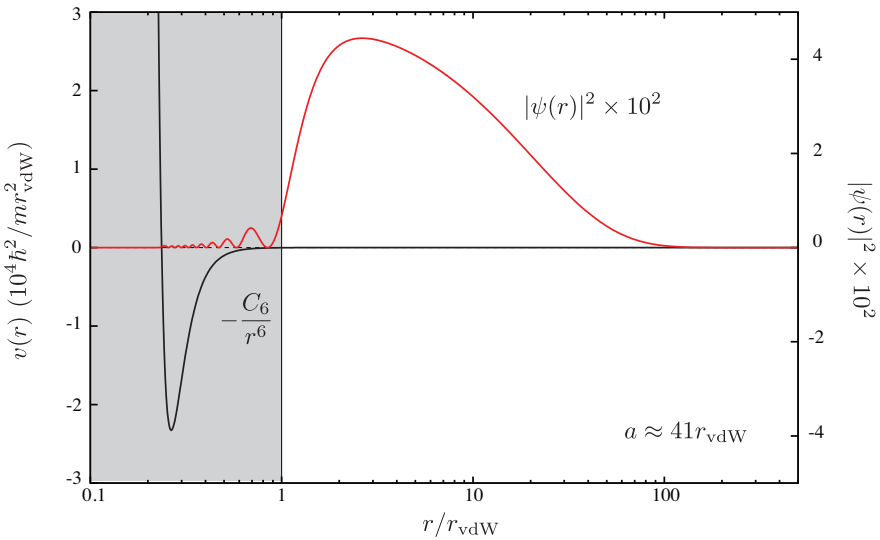

*M. Greiner *et al.*, "Probing pair-Correlated Fermionic Atoms through Correlations in Atom Shot Noise" PRL, **94**, 110401(2005)

Rotations

The high angular velocity of the ISS ($\Omega_{ISS} = 2\pi/91$ min) is considered for:

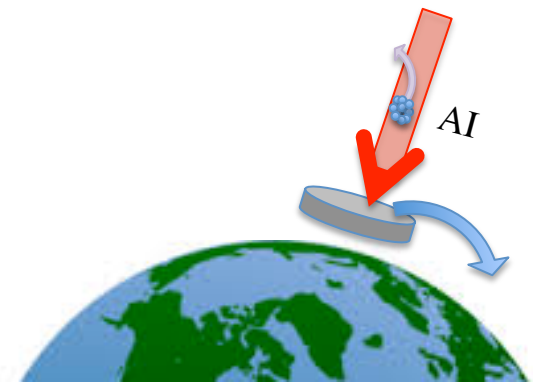

1) Atom drift relative to the Bragg beam: Δx =140 microns at 1s, **not negligible.**

2) Spatial phase fringes due to the Coriolis force. Here, the phase shift for ^{87}Rb at the 1/e thermal width for T = 0.5s and $Temp$ = 1 nK:

$$\Delta\Phi = 2\, \boldsymbol{k}_{eff} (\boldsymbol{\Omega}_{ISS} \times 2k_B Temp/m)\, T^2 = 3.9\ rad$$

- The contrast would be almost completely washed out for this AI without imaging detection[1] or rotation compensation[2]

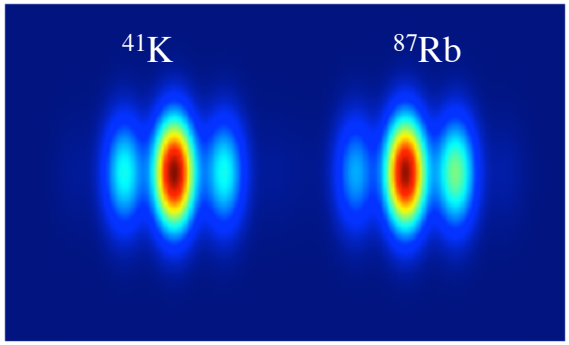

1) Shau-Yu Lan *et al*. "Influence of the Coriolis Force in Atom Interferometry" PRL **108**, 090402, 2012
2) S. Dickerson *et al*. "Multiaxis Inertial Sensing with Long-Time Point Surce Atom Interferometry

Potential Follow-On Studies

Follow-on investigations of the dual-species Feshbach molecule studies:

- Bragg association/dissociation of Feshbach states correlates molecular and motional states

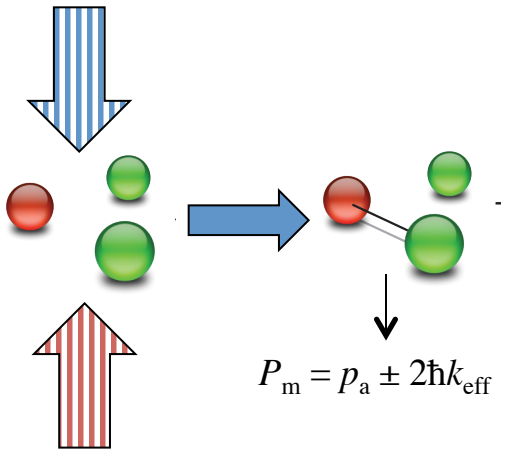

Z. Fu *et al*. (2014) *Nature Physics* **10**, 101

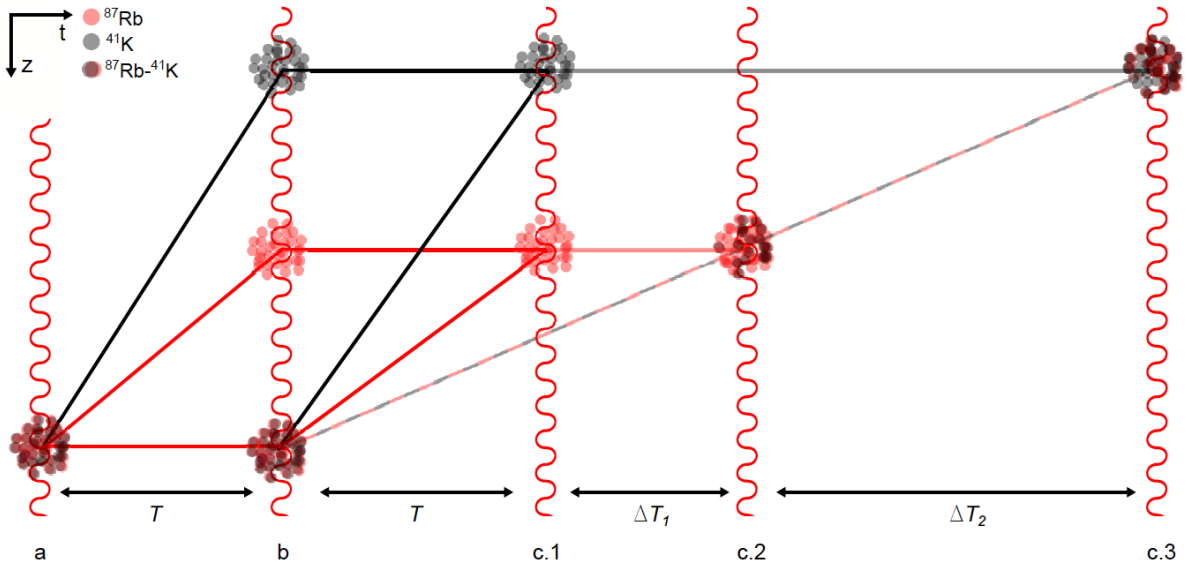

Representative time-space diagram of atom-atom and atom-molecule interferometer topologies with ^{41}K and ^{87}Rb. In each case, the differential wave packets are undergoing a Mach-Zehnder-like interferometer with a series of beamsplitter (a), mirror (b), and recombination (c.1,2,3) pulses. Using weakly-bound molecules as the interferometer input, novel matter-wave interferometer topologies can be explored with atoms and molecules populating the different arms of the interferometers. Dual-species AI with free fall atoms are also shown for reference.